Molecular Biology of the Cell
Vol. 11, 1401–1419, April 2000

EMB-30: An APC4 Homologue Required for Metaphase-to-Anaphase Transitions during Meiosis and Mitosis in *Caenorhabditis elegans*

Tokiko Furuta,* Simon Tuck,† Jay Kirchner,* Bryan Koch,* Roy Auty,*‡ Risa Kitagawa,§ Ann M. Rose,§ and David Greenstein*‖¶

*Department of Cell Biology, Vanderbilt University School of Medicine, Nashville, Tennessee 37232; †Umeå Center for Molecular Pathogenesis, Umeå University, Umeå, Sweden; §Department of Medical Genetics, University of British Columbia, Vancouver, British Columbia, V6T 1Z3 Canada; and ‖The E. Bronson Ingram Cancer Center, Vanderbilt University, Nashville, Tennessee 37232

Submitted December 3, 1999; Revised January 20, 2000; Accepted January 21, 2000
Monitoring Editor: Judith Kimble

Here we show that *emb-30* is required for metaphase-to-anaphase transitions during meiosis and mitosis in *Caenorhabditis elegans*. Germline-specific *emb-30* mutant alleles block the meiotic divisions. Mutant oocytes, fertilized by wild-type sperm, set up a meiotic spindle but do not progress to anaphase I. As a result, polar bodies are not produced, pronuclei fail to form, and cytokinesis does not occur. Severe-reduction-of-function *emb-30* alleles (class I alleles) result in zygotic sterility and lead to germline and somatic defects that are consistent with an essential role in promoting the metaphase-to-anaphase transition during mitosis. Analysis of the vulval cell lineages in these *emb-30(class I)* mutant animals suggests that mitosis is lengthened and eventually arrested when maternally contributed *emb-30* becomes limiting. By further reducing maternal *emb-30* function contributed to class I mutant animals, we show that *emb-30* is required for the metaphase-to-anaphase transition in many, if not all, cells. Metaphase arrest in *emb-30* mutants is not due to activation of the spindle assembly checkpoint but rather reflects an essential *emb-30* requirement for M-phase progression. A reduction in *emb-30* activity can suppress the lethality and sterility caused by a null mutation in *mdf-1*, a component of the spindle assembly checkpoint machinery. This result suggests that delaying anaphase onset can bypass the spindle checkpoint requirement for normal development. Positional cloning established that *emb-30* encodes the likely *C. elegans* orthologue of APC4/Lid1, a component of the anaphase-promoting complex/cyclosome, required for the metaphase-to-anaphase transition. Thus, the anaphase-promoting complex/cyclosome is likely to be required for all metaphase-to-anaphase transitions in a multicellular organism.

INTRODUCTION

Meiosis is a fundamental and conserved biological process required for eukaryotic sexual reproduction. The meiotic process generates a haploid genome (1n) from a diploid genome (2n) by means of two successive divisions, the reductional division (MI) and the equational division (MII), after premeiotic DNA replication and meiotic recombination. Because meiosis is likely to have evolved from mitosis, much of the mitotic machinery is expected to be involved in meiosis. Indeed, cdc2/CDC28, the catalytic subunit of Cdk1, which is genetically well characterized for its role in mitosis, is a component of MPF, which triggers the G2/MI transition in frog oocytes (reviewed by Morgan, 1997).

Although there are similarities between meiosis and mitosis, there are also major differences. Probably the most striking difference in meiosis is that sister chromatids cosegregate while homologues disjoin at MI. In contrast, sister chromatids disjoin at MII and during mitosis. In *Saccharomyces cerevisiae*, a major difference between meiosis and mitosis involves the differential function and regulation of related cohesin subunits. Elimination of sister-chromatid cohesion at anaphase of mitosis has been shown to require the activity of the anaphase-promoting complex/cyclosome (APC/C) and its substrate-specific activator Cdc20p, whose role is to promote the ubiquitin-mediated degradation of the anaphase inhibitor Pds1p (reviewed by Zachariae and

‡ Present address: Department of Pathology, Harvard Medical School, Boston, MA 02115.
¶ Corresponding author. E-mail address: david.greenstein@mcmail.vanderbilt.edu.

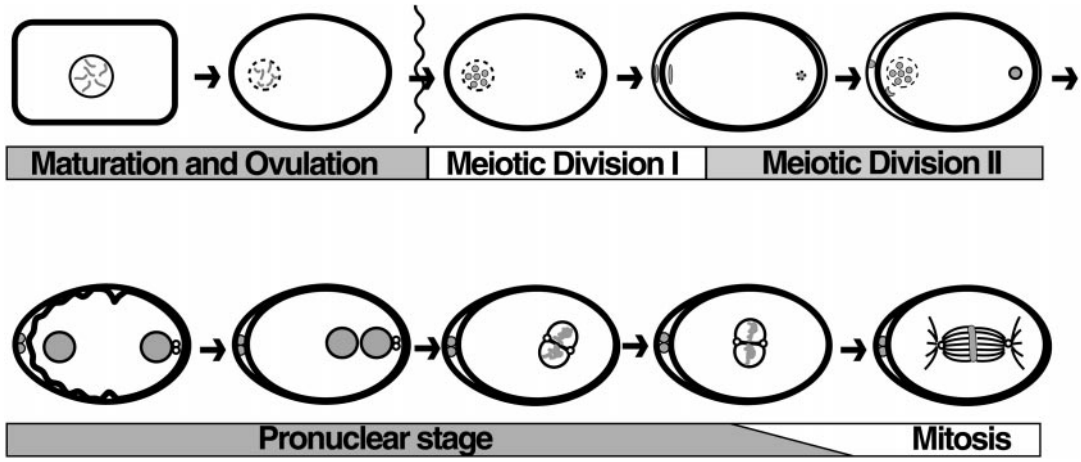

Figure 1. The oocyte meiotic divisions and early embryogenesis. Oocyte meiotic maturation involves nuclear envelope breakdown (meiotic M-phase entry) and cortical rearrangement. The oocyte is fertilized as it enters the spermatheca. The condensed sperm chromatin is shown in the posterior (at right) of the embryo. The MI and MII divisions are completed in the uterus, forming two polar bodies at the anterior. Pronuclei form (bottom left), meet in the posterior, and fuse as they enter mitotic M phase (the small unfilled circles are centrosomes). The time from nuclear envelope breakdown to pronuclear meeting is ~45 min.

Nasmyth, 1999). Ubiquitin-mediated degradation of Pds1p results in the activation of Esp1p and the cleavage of the Scc1p cohesin subunit (Uhlmann *et al.*, 1999). In meiosis, the cohesin subunit Rec8p persists at centromeres until anaphase II, providing a potential mechanism for maintenance of sister-chromatid cohesion during anaphase I (Klein *et al.*, 1999). These recent advances have provided a framework for analyzing the molecular mechanisms underlying the metaphase-to-anaphase transition during meiosis and mitosis, yet many questions still remain (Nasmyth, 1999). For example, it is unclear how the APC/C is assembled and localized, how anaphase is triggered, how substrates are recognized, and how these events are integrated into a developmental context in multicellular organisms.

In our efforts to analyze the developmental control of cell cycle events in a multicellular organism, we focused on the oocyte meiotic divisions in *Caenorhabditis elegans*. The oocyte meiotic divisions provide a convenient experimental system because the oocyte is large, the bivalents are cytologically observable, and the cell cycle events are well described (Ward and Carrel, 1979; Albertson, 1984; Albertson and Thomson, 1993; McCarter *et al.*, 1997; Rose *et al.*, 1997; Hall *et al.*, 1999). *C. elegans* hermaphrodites produce both sperm and oocytes. Sperm are formed during the L4 stage of development, and oocytes during the adult stage. Oocytes remain in the diakinesis stage of prophase I before undergoing meiotic maturation (Figure 1), during which the nuclear envelope breaks down and the oocyte rounds up (cortical rearrangement; McCarter *et al.*, 1999). A sperm-associated signal(s) promotes oocyte meiotic maturation independent of fertilization (McCarter *et al.*, 1999). Nuclear envelope breakdown during meiotic maturation is promoted by the CDK1-related kinase NCC-1 (Boxem *et al.*, 1999), and the oocyte is fertilized as it enters the spermatheca. The meiotic divisions are completed after transfer to the uterus, where embryogenesis ensues (Albertson, 1984; Albertson and Thomson, 1993).

Here we present an extensive genetic, phenotypic, and molecular analysis of the *emb-30* locus. *emb-30* was originally defined by the incompletely penetrant and variably expressed mutation *emb-30(g53*ts*)*, which results in one-cell arrest with one polar body and often multiple nuclei (Cassada *et al.*, 1981; Isnenghi *et al.*, 1983; Denich *et al.*, 1984). Based on the analysis of stronger mutant alleles, we show here that *emb-30* is required for metaphase-to-anaphase transitions during meiosis and mitosis in both the germ line and the soma. Class I *emb-30* alleles cause zygotic sterility and result from a severe reduction in *emb-30* function. Analysis of the vulval cell lineages in these *emb-30(class I)* mutant animals suggests that mitosis is lengthened and eventually arrested when maternally contributed *emb-30* becomes limiting. By further reducing maternal *emb-30* function contributed to class I mutant animals, we demonstrate that *emb-30* is required for the metaphase-to-anaphase transition in many or all cells. Mitotic arrest in *emb-30* mutants reflects an essential role in M-phase progression and is not a secondary consequence of spindle assembly checkpoint activation. We show further that a reduction in *emb-30* function can suppress the lethality and sterility caused by a null mutation in *mdf-1*, the likely *C. elegans* orthologue of the spindle checkpoint gene *MAD1* (Kitagawa and Rose, 1999). This result provides support for the idea that the primary essential role of the spindle assembly checkpoint in *C. elegans* is not in the chromosome segregation process itself but rather in delaying anaphase onset until all chromosomes are properly attached to the spindle. Molecular identification of *emb-30* as the likely *C. elegans* orthologue of APC4/Lid1, a biochemically characterized component of the APC/C, provides direct in vivo evidence that the APC/C is likely to be required for all metaphase-to-anaphase transitions in a multicellular organism. The cell type–specific *emb-30* alleles may provide insight into developmental control of the cell cycle and meiotic/mitotic differences.

MATERIALS AND METHODS

Genetic Techniques, Nematode Strains, and Nomenclature

C. elegans strains were cultured at 20°C (Brenner, 1974) with the following general exceptions. The permissive temperature for all temperature-sensitive (ts) strains was 15–16°C. The restrictive temperature for *emb-30(tn377*ts*)* and *emb-30(ax69*ts*)* was 25°C, and the restrictive temperature for *emb-30(g53*ts*)* was 26°C. Mutagenesis was performed with 50 mM ethyl methanesulfonate (EMS; Brenner, 1974), 1 mM *N*-ethyl-*N*-nitrosourea (ENU; De Stasio *et al.*, 1997), or 30 μg/ml 4,5′8-trimethylpsoralen (TMP) and 340 μW/cm^2 UV light (366 nm) for 1–2 min (Yandell *et al.*, 1994). "Embryo" is used to refer to a fertilized oocyte irrespective of whether the oocyte completes the meiotic divisions. The following *C. elegans* genes, mutations, deficiencies, rearrangements, and extrachromosomal arrays were used (see Hodgkin [1997] for references or as cited): *LGI*: *smg-1(r861)*, *gld-1(q485)*, *fog-3(q443)*, *glp-4(bn2*ts*)*, *unc-54(r293)*; *LGII*: *rol-6(su1006*d*)*, *let-23(sy10)*; *LGIII*: *fem-2(b245*ts*)*, *unc-36(e251)*, *dpy-19(e1259* ts, mat*)*, *sma-2(e502)*, *unc-32(e189)*, *glp-1(q46)*, *emb-9(hc70* sd, ts*)*, *emb-30(ax69*ts*)* (provided by A. Golden, NIDDK, NIH, Bethesda, MD), *emb-30(g53*ts*)*, *emb-30(tn)* alleles (this paper), *sod-4(pk68::Tc1)* (provided by L. Speliotes, MIT, Cambridge, MA), *ced-7(n1892)*, *sqv-3(n2823)*, *unc-69(e587)*; *LGIV*: *fem-3(q20* gf, ts*)*; *LGV*: *fog-2(q71)*, *unc-46(e177)*, *mdf-1(gk2)* (Kitagawa and Rose, 1999); *LGX*: *ceh-18*. Rearrangements, duplications, and deficiencies were as follows: *hT2 [bli-4(e937)]I*; *hT2 [dpy-18(h662)]III*; *hT1(I, V)*, *mnC1[dpy-10(e128) unc-52(e444)]II*; *eT1(III, V)*, *tnDf2* (this work). Extrachromosomal arrays were as follows: *tnEx12*[F54C8 + *rol-6(su1006*d*)*]; *tnEx13* [pBK1 + *rol-6(su1006*d*)*].

Isolation of emb-30 Mutations

*emb-30(tn377*ts*)* was isolated in a large-scale DAPI screen for ts mutations affecting oogenesis. A total of 336 independent ts strains were isolated from 10,357 EMS-mutagenized F2 lines and screened for oocyte defects by differential interference contrast (DIC) microscopy and DAPI staining after transfer of L4- and L1-stage larvae to 25°C. One mutation from this screen, *tn377*ts, blocked the meiotic divisions and germline proliferation, as described in RESULTS. *tn377*ts failed to complement *emb-30(g53*ts*)* for the maternal-effect embryonic lethal phenotype. *emb-30(tn377*ts*)* was outcrossed at least seven times, and linked mutations were removed by recombination.

The rest of the *emb-30(tn)* alleles were isolated in genetic screens for new mutations that failed to complement *emb-30(tn377*ts*)*. In the "trial-by-fire" screen, N2 males were mutagenized and mated to *emb-30(tn377*ts*) ced-7(n1892) unc-69(e587)* hermaphrodites at 16°C. F1 cross progeny were placed individually on Petri plates and allowed to lay eggs for 2–3 d at 16°C. The F1 parent was then transferred to a fresh Petri plate and returned to 16°C, whereas the F2 eggs were placed at 25°C and screened for ts maternal-effect lethality or sterility. In this screen, 11 independent *emb-30* alleles (*tn471–tn481*) were obtained from 10,871 EMS-mutagenized haploid genomes, and *tnDf2* was obtained from 8029 TMP-mutagenized haploid genomes. This F2 clonal screen is biased against the isolation of viable *emb-30* alleles. Nevertheless, viable alleles (*tn474* and *tn481*) were obtained because they were fortuitously linked to lethal mutations that were removed by backcrossing and genetic mapping. To circumvent this bias against viable alleles, we sought additional alleles in the "redemption" screen. In this screen, *unc-32(e189)/unc-36(e251)* males were mutagenized and mated to *sma-2(e502) emb-30(tn377*ts*) ced-7(n1892) unc-69(e587)* hermaphrodites at 16°C. F1 cross progeny were placed individually at 25°C and screened for maternal-effect lethal or sterile-with-oocytes phenotypes. Hermaphrodites displaying either of these phenotypes were mated to wild-type males at 16°C to recover the mutagenized chromosome. This screen takes advantage of the fact that *emb-30(tn377*ts*)* hermaphrodites that lay all dead eggs at 25°C can regain fertility upon transfer to 16°C, especially when mated to wild-type males. *emb-30(tn493)* was obtained from 5275 EMS-mutagenized haploid genomes, and *emb-30(tn494)* was obtained from 3324 ENU-mutagenized haploid genomes.

Each mutation was outcrossed at least seven times, with the exception of *tn493* and *tn494*, which were outcrossed twice. All *emb-30* alleles are recessive to the wild type. Zygotic sterile or Mel alleles were maintained as balanced heterozygous stocks. *emb-30* class I homozygotes showed an incompletely penetrant and variably expressed slow-growth phenotype when *eT1* was used as the balancer chromosome, suggesting that *eT1* may not provide full maternal *emb-30* function. For phenotypic studies, class I homozygotes were maintained heterozygous to *unc-36(e251)*.

*emb-30(tn377*ts*)* was mapped with respect to most *LGIII* marker genes used in this study (data submitted to ACEDB at http://probe.nalusda.gov:8300/cgi-bin/browse/acedb). *emb-30* was further positioned on *LGIII* between *emb-9* and *sod-4* (see RESULTS). *sod-4(pk68::Tc1)* was detected with the use of single-worm PCR (Williams, 1995) with the G3321A primer (5′-CTCGTGACACATATCTGAG-3′) and the R1 primer (Plasterk, 1995), resulting an a 631-base pair (bp) product. The *sod-4(+)* allele was detected with the use of the G3321A primer together with the OMB2 primer (5′-GATTGGTCAACATTCTCTATC-3′), resulting in a 915-bp PCR product. All *emb-30* alleles failed to complement *emb-30(tn377*ts*)* and mapped to this region. *tnDf2* fails to complement all tested *emb-30* mutant alleles *(tn377*ts, *tn471*, *tn472*, *tn474*, *tn477*, *tn479*, *tn481*, *tn494*), *ced-7(n1892)*, and *sqv-3(n2823)*. *tnDf2* complements *unc-36(e251)*, *sma-2(e251)*, *dpy-19(e1259)*, *unc-32(e189)*, *glp-1(q46)*, *emb-9(hc70*ts*)*, and *unc-69(e587)*. *tnDf2/+* heterozygous males are mating defective; thus, all crosses used *tnDf2* heterozygous hermaphrodites purged of sperm or heterozygous strains in which the deficiency was marked by *unc-32(e189)* or *sma-2(e502)*.

Phenotypic Analysis

General techniques for DIC observations of oocyte meiotic maturation, ovulation, and early embryogenesis were as described (Rose *et al.*, 1997). DIC observations of early embryogenesis were made in utero. Cytological analyses were performed as described (Albertson and Thomson, 1993; Nonet *et al.*, 1997; Rose *et al.*, 1997). Cytological analyses of one-cell embryos were performed by dissecting adult hermaphrodites in egg salts (Edgar, 1995) 16 h after transfer of L4 larvae to 25°C. The following antibodies were used: anti-tubulin (Kilmartin *et al.*, 1982; Blose *et al.*, 1984); anti-nuclear pore complex Mab414 (Davis and Blobel, 1986); anti-P-granule OIC1D4 (Strome and Wood, 1982); anti-sperm membrane protein SP56 (Ward *et al.*, 1986); anti-phosphohistone H3 (Mahadevan *et al.*, 1991); anti-centrosome (Strome, 1986); and anti-CEH-18 (Greenstein *et al.*, 1994). Polar bodies were stained with 0.1 μg/ml Hoechst 33342 in egg salts or viewed with DIC microscopy in utero. Endomitotic oocyte formation was analyzed by staining with DAPI (0.2–1 μg/ml) 16 h (25°C) or 40 h (16°C) after L4, as described (Rose *et al.*, 1997).

To analyze the effect of *emb-30(tn377*ts*)* on germline proliferation during postembryonic development, 2-h egg-lays were conducted at 16°C and embryos were transferred to 25°C. Larvae were synchronized by collecting L1-stage animals that hatched in a 1-h period. Developmental stage was analyzed by DIC microscopy (Sulston and Horvitz, 1977). DAPI-stained germ cells were counted in paraformaldehyde-fixed whole-mount preparations. To analyze the effect of *emb-30(tn377*ts*)* on germ cell mitosis in the distal mitotic zone of the adult hermaphrodite gonad, worms were grown at 16°C, synchronized as described above, and shifted to 25°C as young adults (92 h after hatch at 16°C). Gonads were dissected and fixed (0, 2, 4, 8, 12, 18, and 24 h after shift), and mitotic cells were visualized with anti-phosphohistone H3 antibodies. To analyze germline proliferation in *emb-30* class I sterile alleles, L4-stage or adult (13 h after L4 at 20°C) gonads were dissected and stained as described above.

The vulval cell lineages were analyzed as described (Sternberg and Horvitz, 1989). To analyze somatic phenotypes of *emb-30* class I alleles under conditions in which maternally contributed *emb-30*

was reduced, we examined the progeny of DG823 *unc-32(e189) emb-30(class 1)/sma-2(e502) emb-30(tn377*ts*) ced-7(n1892) unc-69(e587)* hermaphrodites. Larval phenotypes were examined 24 h after embryos were shifted from 16 to 25°C. Early embryonic phenotypes were examined both 24 h after embryos were shifted from 16 to 25°C and 2 h after embryos were shifted from 20 to 25°C. After the temperature shift, arrested embryos and larvae were observed. Arrested larvae were Unc-32 or paralyzed and were recognized by their translucent appearance. Unc-32 sterile adults were not observed among the animals surviving to adulthood after the temperature shift. Arrested embryos were recognized by the failure of embryonic cell division. Mitotic nuclei were counted in picric acid–fixed preparations (Nonet *et al.*, 1997) stained for phosphohistone H3, tubulin, and DNA.

Molecular Analysis of emb-30

The left breakpoint of *tnDf2* was mapped by PCR of homozygous-deficiency embryos and Southern analysis of DG802 *unc-32(e189) tnDf2/unc-32(e189) glp-1(q46)*. RNA interference (RNAi) was performed as described (Fire *et al.*, 1998). For transgenic rescue experiments (Mello and Fire, 1995), PCR was used to generate a 9.9-kilobase (kb) clone (pBK1) containing 3 kb upstream of the *emb-30* initiator methionine and a frame shift in F54C8.1. F54C8 (1 μg/ml) or pBK1 (10 μg/ml) was coinjected with pRF4[*rol-6(su1006*d*)*] (50 μg/ml; Kramer *et al.*, 1990) into *unc-32(e189) emb-30(tn475)/unc-36(e251)* hermaphrodites. The phenotypes of ~20 Unc-32 Rol progeny per F2 line were analyzed, with Unc-32 non-Rol progeny serving as a control. For reverse transcription (RT)-PCR experiments to map the 5′ end of the *emb-30* message, first-strand cDNA was prepared from 10 μg of poly(A)+ RNA with the use of the Superscript preamplification system (Life Technologies/BRL, Grand Island, NY). PCR was performed with SL1 and SL2 primers (Krause, 1995) and multiple *emb-30* primers. A single 5′ end was detected by sequencing RT-PCR products and verified by sequencing cDNA clones. *emb-30* RNA expression was analyzed by Northern blot hybridization to poly(A)+ RNA with the use of cDNA probes. To normalize RNA loading, the blot was stripped, rehybridized to a *ceh-18* cDNA probe, and quantitated with the use of a Molecular Dynamics (Sunnyvale, CA) PhosphorImager.

Pooled PCR fragments, amplified from individual worms, were sequenced on both strands. DNA sequencing of genomic DNA and cDNA clones indicated an omission of a single C residue at position 4500 of F54C8, resulting in an alteration to the Genefinder (L. Hillier and P. Green, personal communication) prediction. This change has been submitted to ACEDB; however, we mention it here so that others may avoid difficulties that can arise with the use of the incorrect F54C8.3 prediction. Protein sequences were analyzed with the use of the BLAST algorithm (Altschul *et al.*, 1997) and the Genetics Computer Group (Madison, WI) sequencing package. Amino acid alignments of EMB-30 with human APC4 and *Schizosaccharomyces pombe* Lid1 were generated with the use of the CLUSTAL W algorithm (Thompson *et al.*, 1994). WD-repeat sequences were aligned with the use of the PileUp program (Genetics Computer Group, Madison, WI), with manual alterations made after inspection.

RESULTS

emb-30 Is Required for Completion of the Meiotic Divisions

We sought ts mutations that result in abnormalities in the completion of the meiotic divisions. A screen for ts mutants permits the isolation of genes required for oogenesis that also have roles earlier in development. One mutation from this screen, *emb-30(tn377*ts*)*, was particularly striking in that it blocked the meiotic divisions of both oocytes and sperm as well as germline proliferation. At the nonpermissive temperature, *emb-30(tn377*ts*)* mutants exhibit a completely penetrant maternal-effect lethality, with all embryos arresting at the one-cell stage (Figures 2 and 3; Table 1). Similar results were obtained when embryos were produced by mating *fog-2(q71)I emb-30(tn377*ts*)* females with wild-type males (Figure 3C; Table 1). The *fog-2* mutation feminizes the germ line of XX animals so that they do not produce sperm, ensuring that all embryos result from cross-fertilization and are of genotype *emb-30(tn377*ts*)/+*. DIC microscopic observations indicated that oocyte meiotic maturation (nuclear envelope breakdown and cortical rearrangement) and ovulation occurred normally. Three observations suggested that the ovulated oocytes were in fact fertilized: 1) they produced eggshells; 2) the sperm chromatin could be observed within the embryo by DAPI staining (Figure 2L); and 3) the embryos stained with the sperm-specific mAb SP56 (Figure 2K). Polar body formation was significantly reduced at the nonpermissive temperature [3% (n = 185) for *emb-30(tn377*ts*)* and 1% (n = 126) for *fog-2(q71); emb-30(tn377*ts*)* females mated to wild-type males], suggesting a defect in completing the meiotic divisions. Consistent with this possibility, several postmeiotic events did not occur: 1) pronuclei did not form, as detected by DIC microscopy or with a nuclear pore complex antibody (Figure 3I; n = 201); 2) pseudocleavage, and the anterior cortical contractions that generate posteriorly directed cytoplasmic flows at pseudocleavage, did not occur; 3) P-granules, putative germline determinants, did not coalesce or segregate; and 4) cytokinesis was absent. These results are consistent with the hypothesis that *emb-30(tn377*ts*)* mutant embryos are defective in completing the meiotic divisions and that the origin of this meiotic defect can be attributed to the oocyte.

To elucidate the basis for the meiotic defect, we conducted a cytological analysis of spindle and chromatin morphology after fertilization (Figures 2, A–J, and 3C; Table 1). In our wild-type sample (n = 895), 18% (n = 158) of the embryos were at the one-cell stage, and these were distributed as expected between MI (23%; n = 37), MII (33%; n = 52), pronuclear stage (29%; n = 45), and the first mitosis (15%; n = 24). During MI (Figure 2A) and MII, an acentriolar barrel-shaped spindle assembles adjacent to the anterior cortex surrounding the maternal DNA. In contrast, wild-type pronuclear-stage embryos in prophase of the first mitotic division assemble a mitotic spindle with centrosomes and asters (Figure 2C). In sharp contrast to these results in the wild type, *emb-30(tn377*ts*)* mutant oocytes fertilized at the nonpermissive temperature were all (n = 353) in a meiotic stage (Table 1). Because polar body formation was rare, these one-cell embryos likely represented arrest at MI. The spindle morphology exhibited by the meiotically arrested *emb-30(tn377*ts*)* embryos was variable (Figures 2, E, G, and I, and 3C; Table 1). There was a distribution of meiotic spindle types, from cortically localized barrel-shaped spindles (Figure 2E; Table 1), to mislocalized barrel-shaped spindles (Figure 3C), to disorganized meiotic spindles (Figure 2G), in which enlarged microtubule masses surrounded meiotic chromatin that was not located adjacent to the anterior cortical membrane. A failure to stain with anti-centrosome antibodies verified that the disorganized spindles were acentriolar meiotic spindles (our unpublished results). Likewise, the meiotic chromatin morphology displayed a distri-

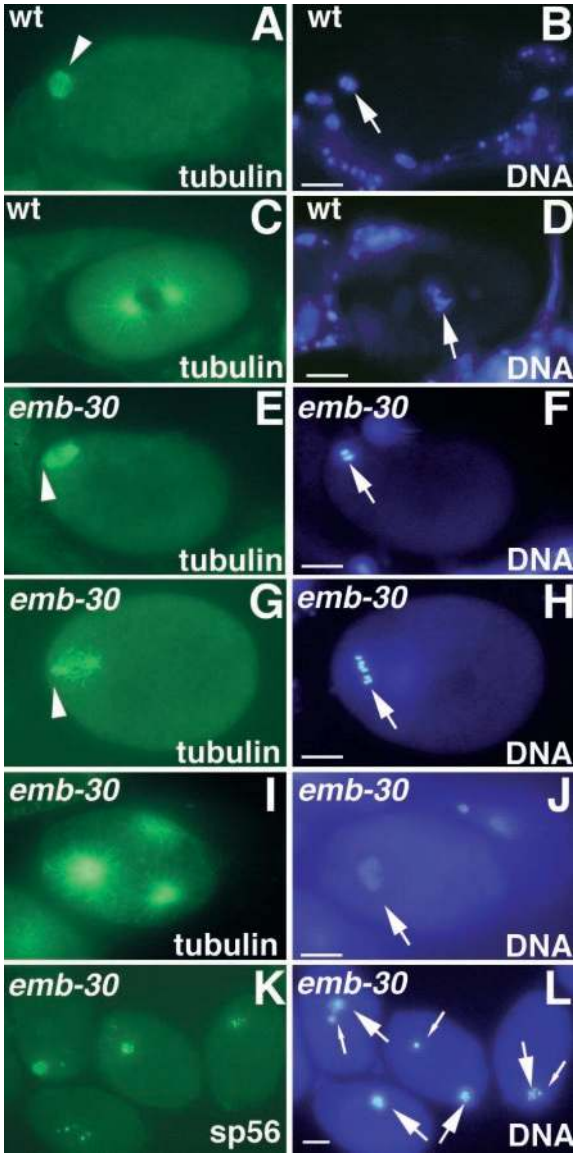

Figure 2. *emb-30* is required for completion of the oocyte meiotic divisions. Cytological analysis of embryos stained for tubulin, a sperm membrane protein (sp56), or DNA, as indicated. Wild-type (A and B) and *emb-30(tn377*ts*)* (E and F) embryos in MI metaphase. The MI spindle (arrowheads) is associated with the anterior cortex. (C and D) Wild-type pronuclear-stage embryo in prometaphase of the first mitotic division. (G and H) *emb-30(tn377*ts*)* one-cell embryo with a disorganized meiotic spindle (arrowhead). Six bivalents are visible (arrow), but there is no evidence of chromosome segregation. The spindle and chromatin are not closely associated with the anterior cortex. This particular spindle and chromatin morphology is not observed in the wild type. (I and J) *emb-30(tn377*ts*)* one-cell embryo with multipolar spindles. Three microtubule-organizing centers are seen. (K and L) *emb-30(tn377*ts*)* one-cell embryos stain for a sperm membrane protein and contain both maternal DNA (large arrows) and paternal DNA (small arrows). It is unclear how the female and male chromatin can on occasion come to be adjacent in the arrested embryos. This does not reflect nuclear migration processes because pronuclei do not form. Bars, 10 μm.

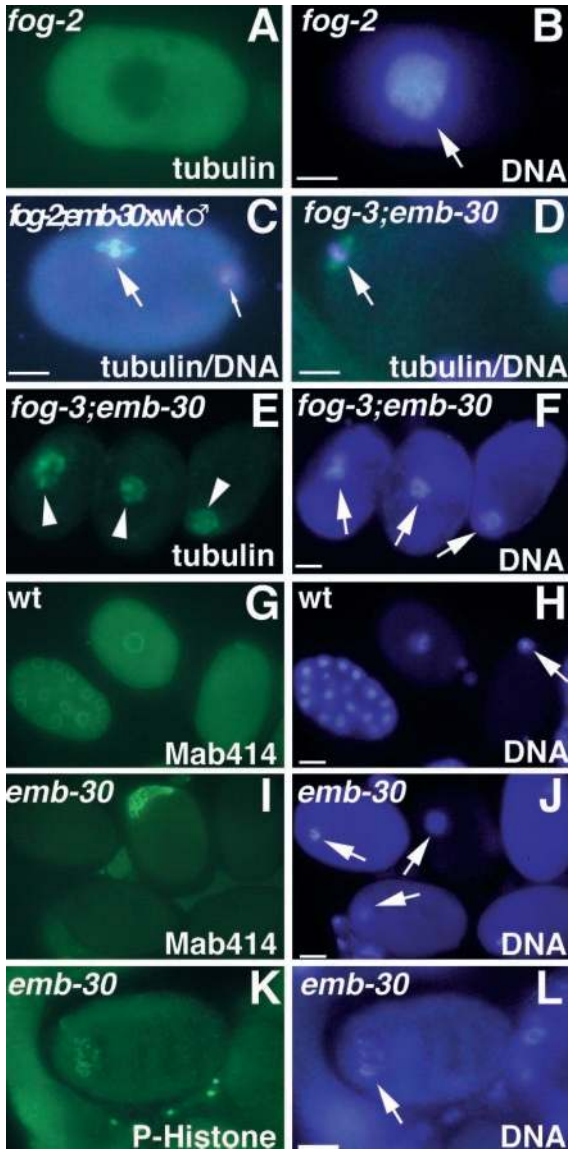

Figure 3. Cytological analysis of embryos or oocytes stained for tubulin, nuclear pore complex (Mab414), phosphohistone H3 (P-Histone), or DNA, as indicated. (A and B) Unfertilized oocyte from a *fog-2* female showing intense DAPI staining (arrow) and diffuse tubulin staining. (C) One-cell embryo after fertilization of a *fog-2; emb-30(tn377*ts*)* oocyte with wild-type sperm. The MI spindle (large arrow) is in metaphase but is not associated with the anterior cortex. The paternal DNA is in the posterior (small arrow) but slightly out of the plane of focus. (D) Unfertilized oocyte from a *fog-3; emb-30(tn377*ts*)* female. An MI spindle can assemble in the absence of fertilization (arrow) and associate with the anterior cortex, but the oocyte does not become endomitotic. (E and F) Unfertilized oocytes from *fog-3; emb-30(tn377*ts*)* females. Disorganized meiotic spindle–like structures (arrowheads) associate with the maternal chromatin (arrows). Note that there are three separate oocytes in panels E and F. (G and H) Wild-type embryos form nuclear envelopes. Gastrula-stage embryo (left), pronuclear-stage embryo (middle), and meiotic embryo (right). (I and J) In *emb-30(tn377*ts*)*, there is no indication of nuclear envelope formation. Instead, an amorphous aggregate of nuclear pore complex material is found in 8% of the arrested embryos. Maternal DNA is indicated by arrows. (K and L) Less condensed chromatin (arrow) contains phosphohistone H3, indicating that the embryo arrests in M phase. Bars, 10 μm.

Table 1. Cytological distribution of *emb-30(tn377*ts*)* embryos

Parental genotype	Chromatin morphology[a]	Spindle morphology				n
		Meiotic[b]	Disorganized[c]	Multipolar[d]	No staining[e]	
*emb-30(tn377*ts*)*	Condensed DNA	20%	25%	2%	3%	175
	Less condensed DNA	1%	31%	16%	3%	178
	Total					353
*fog-2(q71); emb-30(tn377*ts*)* ♀ × wild-type ♂	Condensed DNA	12%	9%	0%	1%	73
	Less condensed DNA	0%	53%	17%	8%	264
	Total					337

Embryos were dissected from adult worms 16 h after transfer to 25°C. The cytology of the meiotic spindle and chromatin was analyzed in fixed samples stained with anti-tubulin antibodies and DAPI (see MATERIALS AND METHODS). All meiotic stages were observed in the wild-type control (see RESULTS). In contrast, not all meiotic stages were observed in the one-cell arrested *emb-30(tn377*ts*)* embryos. The last stage that appeared normal was meiotic metaphase I.

[a] Chromatin morphology was scored as condensed if the DAPI-staining bivalents appeared compacted, as in the wild type. Other morphologies were scored as less condensed. The less condensed morphology included both subtle deviations from the wild type and gross alterations in which the chromatin had a stringy appearance and was spread out in the center of the cell.

[b] The spindle morphology was scored as meiotic if the acentriolar meiotic spindle had a barrel shape that was within the range of structures visualized in the wild type.

[c] Disorganized spindles included those in which a bipolar structure was still evident and those in which the spindle was a cloud of tubulin surrounding the chromatin.

[d] The multipolar designation was given to spindles in which the tubulin-staining structures were centrosomes with asters. Multipolar spindles were seen irrespective of the genotype of the sperm. The multipolar spindles are inferred to arise from duplication of the sperm centrosome and not polyspermy, because we did not observe more than one major focus of condensed sperm chromatin.

[e] No tubulin staining included cases in which the spindle was likely to have been disassembled or the embryo was not properly permeabilized. In either case, this was a small fraction of the total sample and was unlikely to affect the conclusions drawn.

bution from normal-looking, condensed meiotic bivalents congressed on the metaphase plate at the anterior cortex (Figure 2F) to less condensed chromatin located within the interior (Figures 2J and 3L). The less condensed chromatin morphology was associated with a disorganized spindle morphology (Table 1). Significantly, we did not observe a clear separation of the maternal homologous chromosomes or sister chromatids (n = 690), suggesting that anaphase I did not occur normally. For example, in Figure 2, G and H, the six bivalents and a disorganized spindle are visible, but there is no evidence of chromosome segregation. Based on these results, we suggest that *emb-30(tn377*ts*)* mutant embryos are defective in the metaphase-to-anaphase transition of MI. Nevertheless, we observed evidence for the limited execution of at least one postmeiotic event. Approximately 17% of the arrested *emb-30(tn377*ts*)* mutant embryos set up multipolar spindles in which the sperm centrosome divided a few times and nucleated asters (Figure 2I; Table 1). However, these multipolar spindles did not associate with chromatin, and there was no apparent kinetic activity.

Because oocytes undergo meiotic maturation in spatial-temporal sequence, such that the younger embryos are found in the most distal portion of the uterus, we could superimpose a plausible temporal order on our cytological observations. When *emb-30(tn377*ts*)* embryos were analyzed in utero by DAPI staining at the nonpermissive temperature, the one-cell embryos located in the distal portion of the uterus generally had normal-appearing condensed chromatin, whereas the proximally located one-cell embryos had less condensed chromatin. Thus, as the arrested embryos age, it is likely that the chromatin becomes less condensed and the spindle becomes disorganized. Importantly, antibody staining indicated that the meiotic chromatin of the arrested embryos contained phosphorylated histone H3, an M-phase marker (Figure 3, K and L; our unpublished results), even in instances in which the chromatin was less condensed. This result suggests that the mutant embryos are unable to exit M phase of the meiotic cell cycle.

To examine whether the meiotic cell cycle block observed in *emb-30(tn377*ts*)* at the nonpermissive temperature could occur in the absence of fertilization, we analyzed *emb-30(tn377*ts*); fog-2(q71)* and *fog-3(q443); emb-30(tn377*ts*)* double mutants. These *fog* mutations result in the production of oocytes only, which undergo meiotic maturation at a low rate (McCarter *et al.*, 1999) but are not fertilized without mating to males. These ovulated but unfertilized oocytes cycle between S and M phases, without cytokinesis or karyokinesis, becoming highly polyploid (Ward and Carrel, 1979). Unfertilized oocytes ovulated by *fog-2(q71)* or *fog-3(q443)* females become endomitotic and generally stain diffusely with anti-tubulin antibodies (Figure 3, A and B; our unpublished results). In contrast, unfertilized oocytes ovulated by *fog-2(q71); emb-30(tn377*ts*)* or *fog-3(q443); emb-30(tn377*ts*)* females at the nonpermissive temperature do not become endomitotic and arrest with an assembled MI spindle or with a cloud of tubulin surrounding the chromatin (Figure 3, D–F; Table 2). Thus, unfertilized oocytes produced by these *fog; emb-30(tn377*ts*)* females can progress to MI metaphase, but not further. We have not observed meiotic spindles in *fog-2* (or *fog-3*) females; however, they may be transient structures before endomitosis. Similarly, mutations that block ovulation but not meiotic maturation cause the forma-

Table 2. *emb-30(tn377ts)* blocks endomitotic oocyte formation

Parental genotype	Temperature	Emo[a]	Non-Emo[a]
fog-2(q71) ♀[b]	25°C (n = 67)	100%	0%
fog-2(q71); emb-30(tn377ts) ♀[b]	16°C (n = 80)	88%	12%
	25°C (n = 192)	0%	100%
fog-3(q443) ♀[b]	25°C (n = 69)	100%	0%
fog-3(q443); emb-30(tn377ts) ♀[b]	16°C (n = 118)	97%	3%
	25°C (n = 246)	1%	99%
let-23(sy10)[c]	25°C (n = 38)	100%	0%
let-23(sy10); emb-30(tn377ts)[c]	16°C (n = 64)	91%	9%
	25°C (n = 110)	0%	100%

[a] Adult hermaphrodites were analyzed by DAPI staining and scored with regard to whether they contained endomitotic oocytes (Emo).
[b] Oocytes were ovulated and were scored in the uterus for the endomitotic-oocyte phenotype.
[c] Endomitotic oocytes were scored in the gonad arm.

tion of endomitotic oocytes in the gonad arm [e.g., *let-23(sy10)*; J. McCarter, B. Bartlett, T. Dang, R. Hill, M. Lee, and T. Schedl, personal communication]. *emb-30(tn377ts)* is also epistatic to *let-23(sy10)* for the endomitotic oocyte phenotype at the nonpermissive temperature (Table 2). Together, these observations strongly suggest that the one-cell-arrest phenotype observed in *emb-30(tn377ts)* mutants is caused by a defect in cell cycle progression and does not reflect a failure of fertilization, or postfertilization activation, to occur properly.

In contrast to those in oocytes, the meiotic spindles in spermatocytes contain centrioles and asters (Albertson and Thomson, 1993). MI results in the formation of two secondary spermatocytes from a primary spermatocyte, and MII results in the formation of four spermatids and a residual body from the two secondary spermatocytes. The residual body contains discarded cellular constituents that are presumably not needed within the sperm. When *emb-30(tn377ts)* larvae are shifted to the nonpermissive temperature at the L3/L4 molt, before spermatogenesis, primary spermatocytes are unable to complete the meiotic divisions, residual bodies do not form, and sperm are not produced. Stronger *emb-30* mutant alleles also fail to complete the meiotic divisions during spermatogenesis (see below). If older *emb-30(tn377ts)* L4 larvae are transferred to the nonpermissive temperature after spermatogenesis has begun, DNA segregation is blocked, but some anucleate sperm and residual bodies form. These sperm apparently can fertilize oocytes, because we often observe fertilized eggs that do not contain the paternal chromatin under these conditions (our unpublished results). This anucleate-sperm phenotype is the predominant phenotype in the weaker ts allele *emb-30(g53ts)* (Sadler and Shakes, 2000; our unpublished results).

emb-30 Is Required for Germline Proliferation

A mitotic role for *emb-30* in germline development was revealed by allowing *emb-30(tn377ts)* hermaphrodites to lay eggs at the permissive temperature and transferring the gastrula-stage eggs to the nonpermissive temperature. These embryos grow into sterile adults that exhibit a strong germline-proliferation-defective (Glp) phenotype, producing at most two germ cells and no gametes (Figure 4A). Both hermaphrodites and males are affected. These sterile adults are otherwise healthy, and somatic structures such as the vulva and the somatic gonad apparently develop normally. This strong Glp phenotype is partially rescued by a maternal wild-type allele, because homozygous *emb-30(tn377ts)* progeny produced from heterozygous mothers at 25°C produce 108 ± 28 (SD) germ cells per gonad arm at the young adult stage (n = 11), compared with 601 ± 72 germ cells per gonad arm in the wild type (n = 11). However, this strong Glp phenotype does not exhibit a strict maternal effect, because *emb-30(tn377ts)/+* cross progeny of *emb-30(tn377ts)* hermaphrodites and wild-type males are non-Glp. Thus, both maternal and zygotic *emb-30* activities contribute to germline proliferation. A striking phenotype is observed in hermaphrodites homozygous for a null mutation in the *gld-1* tumor-suppressor gene: pachytene-stage meiotic germ cells that are specified in the female mode (i.e., those destined to become oocytes) reenter the mitotic cell cycle and form a germline tumor (Francis *et al.*, 1995). The Glp phenotype conferred by *emb-30(tn377ts)* is epistatic to the *gld-1* germline-tumorous phenotype (our unpublished results). Thus, *emb-30* is required for completion of normal and ectopic mitoses in the germ line.

To determine the basis for this Glp phenotype, we examined the time course of germline proliferation during postembryonic development (Figure 4A). At 16°C, germline proliferation is essentially normal in *emb-30(tn377ts)*. In contrast, at 25°C, the germline precursor cells, Z2 and Z3, block in mitosis of their first division during the L1 stage and remain attached at the center of the gonad. Observations made with DIC microscopy and DAPI staining established that nuclear envelope breakdown occurred for both Z2 and Z3 and that a metaphase plate was formed. However, anaphase, cytokinesis, and nuclear envelope reformation did not occur. Thus, *emb-30* is likely to be required for the mitotic division of germ cells.

To determine whether *emb-30* is continually required for germline proliferation, we analyzed the effect of *emb-30(tn377ts)* in the distal mitotic zone of the adult hermaphrodite gonad (Figure 4, B and C). Worms were grown at 16°C and shifted to 25°C as young adults, and mitotic germ cells were visualized by staining with anti-phosphohistone

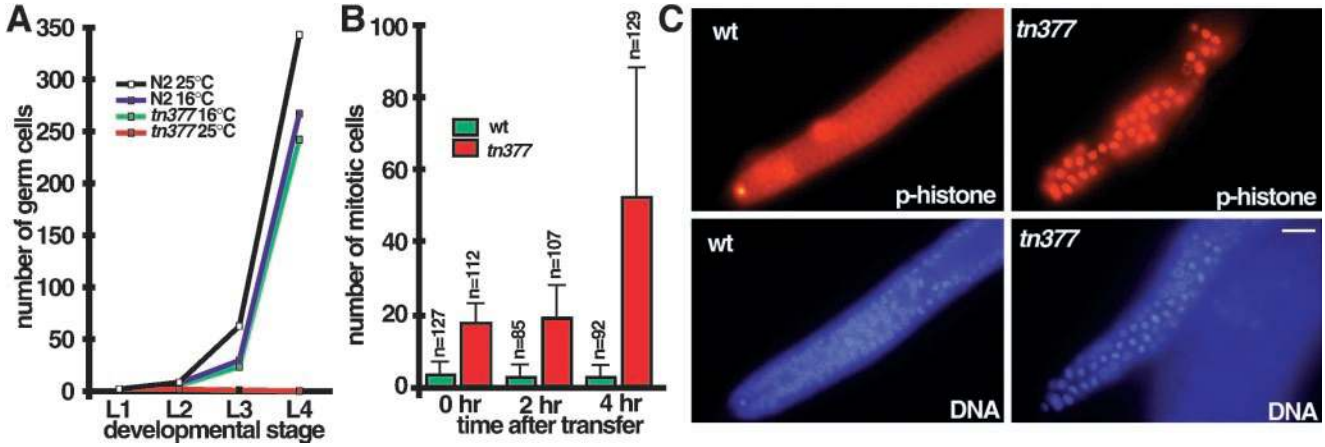

Figure 4. *emb-30* is required for germline proliferation. (A) Time course and temperature sensitivity of germline proliferation in *emb-30(tn377*ts) compared with the wild type. Larvae were synchronized by collecting L1-stage animals that hatched during a 1-h period. Germ cell number per gonad (L1 and L2) or per gonad arm (L3 and L4) was determined at 16 and 25°C. After transfer of gastrula-stage embryos to 25°C, Z2 and Z3 block in mitosis of their first division during the L1 stage; thus, at most, two germ cells are observed. At the L4 stage, germ cells were often absent (0.2 ± 0.5 germ cells per gonad arm; n = 22 gonad arms scored). For the L3 time point, the larvae in the wild-type 25°C sample were at a developmentally later stage (late L3), accounting for the slight increase in germ cell number compared with the 16°C samples. (B and C) Mitotic germ cell accumulation in the distal zone of the *emb-30(tn377*ts*)* adult hermaphrodite gonad. *emb-30(tn377*ts*)* and wild-type hermaphrodites were grown at 16°C and shifted to 25°C as young adults (92 h after hatch at 16°C). Quantitation of mitotic nuclei (mean ± SD; n = number of gonad arms scored at each time point) is shown in B, and representative phosphohistone H3 and DAPI immunofluorescence images from the 4-h time point are shown in C. Bar, 10 μm.

H3 antibodies and DAPI. In *emb-30(tn377*ts*)* gonad arms, there is a significantly increased number of mitotic cells in the distal arm even at the permissive temperature compared with the wild type (Figure 4B, 0 h), suggesting that germ cell mitosis in *emb-30(tn377*ts*)* is slowed at 16°C. By 4 h after transfer to the nonpermissive temperature, mitotic germ cells accumulate in the distal arm (Figure 4, B and C). Metaphase figures were observed by staining with anti-phosphohistone H3 and anti-tubulin antibodies, but anaphase and telophase figures were rare (Figure 4C; our unpublished results). At later times (8–24 h), mitotic chromatin from nearby germ cells becomes intermingled, the distal arm becomes highly disorganized, but total germ cell number does not increase (our unpublished results). Based on these analyses of *emb-30(tn377*ts*)*, we conclude that *emb-30* function is required for germ cells to proliferate mitotically and for oocytes and spermatocytes to complete the meiotic divisions. Furthermore, *emb-30* is likely to be required for the metaphase-to-anaphase transition in these biological processes involving germ cells.

emb-30(class I) Alleles Result in Metaphase-to-Anaphase Transition Defects in the Germ Line and the Soma

The germline specificity of *emb-30(tn377*ts*)* is striking. One possibility is that *emb-30* is germline specific in its functions. An alternative hypothesis is that *emb-30* has both germline and somatic functions but that the germ line is more sensitive to the effects of the *emb-30(tn377*ts*)* mutant allele. To choose between these alternatives, we isolated additional alleles in genetic noncomplementation screens (Table 3). Nine recessive alleles constitute phenotypic class I and result in a completely penetrant zygotic-sterile phenotype (Figure 5, C, D, and H; Table 3). Class I alleles did not exhibit embryonic lethality, because *unc-32(e189)emb-30(tn475)/unc-36(e251)* heterozygotes segregated 25% Unc-32 progeny (619 of 2439 total progeny) that grew to the adult stage and were sterile (n = 619 sterile animals of 619 animals examined). Class I alleles also confer somatic defects, including a vulvaless or everted-small-vulva phenotype (n = 619 of 619 animals scored), a somatic gonadal defect (absence of gonadal sheath cells, spermatheca, and uterus; n = 52 of 52 gonad arms examined), and a severe male tail defect (Figure 5, H and J; n = 67 of 67 males examined). Based on these results, we conclude that *emb-30* has both germline and somatic functions.

To understand better the basis for the *emb-30(class I)* germline-defective phenotypes, we analyzed the development of the germ line and the somatic gonad by DIC microscopy, DAPI staining, and immunocytochemistry. At hatching, the two germline precursor cells, Z2 and Z3, appear normal. Germ cells are able to proliferate mitotically in the early larval stages (L1–L3); however, late during the L3 stage, germ cells in the distal mitotic zone begin to block in mitosis. In the L4 stage, the distal mitotic zone is filled with mitotic nuclei (Figure 5, C and D). In the adult stage, there are 100 ± 15 germ cells in each gonad arm (n = 29 gonad arms examined), a marked reduction compared with the wild type (500–700). In the adult stage, the mitotically blocked germ cells in the distal arm become disorganized. Eventually, the mitotic stem cell population in the distal arm appears to be lost, such that no germ cells are observed at the distal tip (our unpublished results). The first germ cells develop as primary spermatocytes and express a sperm membrane protein as in the wild type (our unpublished results). However, the spermatocytes are unable to complete the meiotic divi-

Table 3. *emb-30* alleles

Class	Alleles[a]	Phenotype
I	*tn471*[b], *tn472*[b], *tn473*, *tn475*[b], *tn476*[b], *tn478*, *tn479*, *tn480*[b], *tn493*	Zygotic sterile; germline and somatic metaphase-to-anaphase transition defects
II	*tn477*	Maternal-effect lethal; embryos arrest at the one-cell stage and fail to complete the metaphase-to-anaphase transition during MI; *smg* suppressible
III		
A	*tn377*ts[b]	Maternal-effect lethal at 25°C; temperature-shifted embryos show defects in germline proliferation (Glp); germ cells fail to complete the metaphase-to-anaphase transition during meiosis or mitosis
B	*g53*ts[c], *ax69*ts[c]	Meiosis defective; incompletely penetrant and variably expressed
IV		
A	*tn481*	Viable; some sterility; fails to complement *tn377*ts for Mel and Glp phenotypes at 25°C
B	*tn474*[d], *tn494*[e]	Viable; fails to complement *tn377*ts for the Mel phenotype, but complements for the Glp phenotype.
V	*tnDf2*	Embryonic lethal[f]

[a] References: *tn* alleles (this work); *g53*ts (Cassada *et al.*, 1981); *ax69*ts (Wallenfang, Seydoux, Shakes, and Golden, personal communication). The molecular lesions in the mutant alleles are shown in Figure 7. Seven maternal-effect lethal mutations described initially as *emb-30* alleles (*t1446*, *t1450*, *t1497*, *t1593*, *t1600*, *t1615*, *t1617*; Gönczy *et al.*, 1999) were misassigned (our unpublished results; Schnabel, personal communication).

[b] Tested and found not to be *smg* suppressible.

[c] The original *emb-30(g53*ts*)*-containing strain (GG53) was described as having an Unc phenotype at 16°C (Cassada *et al.*, 1981). After outcrossing, this phenotype was not observed.

[d] The Mel phenotype of *tn474/tn377*ts heterozygotes is *smg* suppressible.

[e] The Mel phenotype of *tn494/tn377*ts heterozygotes is incompletely penetrant.

[f] Deletes *emb-30*, *ced-7*, and *sqv-3* (see Figure 6).

sions; thus, no sperm are formed (n = 29 gonad arms examined). Likewise, in males, primary spermatocytes are generated, but no sperm form (n = 67 of 67 males examined). Cytological analysis suggests that the primary spermatocytes block at the metaphase-to-anaphase transition of MI (our unpublished results).

Similarly, at hatching, the two somatic gonadal precursor cells, Z1 and Z4, appear normal in *emb-30(class I)* alleles. The distal tip cells are generated in the L1 stage in all animals (n = 52 of 52 gonad arms examined) and are able to exert their leader function necessary for the elongation and migration of both gonad arms. In addition, the distal tip cells are able to promote germline mitosis. The Z1 and Z4 descendants generate the somatic gonad primordium, and the germ cells are rearranged into the developing anterior and posterior gonad arms. However, further division of the somatic gonadal precursor cells is abnormal. Nuclear envelope breakdown occurs, signifying M-phase entry; however, cytokinesis and nuclear envelope reformation do not occur. Staining with anti-phosphohistone H3 antibodies suggested that many somatic gonadal cells blocked in mitosis (our unpublished results). In some cases, we found evidence that a few divisions were able to occur beyond the 12-cell stage. However, in these cases, a spermatheca, uterus, and gonadal sheath were not generated. Significantly, we never observed more than one cell, the distal tip cell, expressing the POU homeoprotein CEH-18 in the gonad (n = 52 gonad arms examined). Because the gonadal sheath cells also express CEH-18, they were apparently not generated.

Vulval development in *emb-30(class I)* alleles is abnormal (Figure 5, compare G and H). DIC observations indicated that the vulval precursor cells (VPCs) were induced by the anchor cell but that the full set of vulval cell divisions was not completed. To understand the nature of this vulval defect, we analyzed the vulval lineages in 10 *unc-32(e189) emb-30(tn475)* animals. The results of this analysis suggest that the vulval defect is caused by an M-phase cell division defect: M phase is considerably lengthened in some divisions, whereas others are never completed. We observed that the nonvulval P3.p, P4.p, and P8.p divisions occurred, although mitosis was considerably lengthened, taking as much as 2 h, compared with ~20 min in the wild type. P5.p, P6.p, and P7.p entered M phase slightly later (as they do in the wild type), but the nuclei of their immediate progeny never appeared. Some time later, variable numbers of hypodermal-looking cells appeared in the ventral cord that appeared to be Pn.pxx cells, i.e., the cells formed in wild-type animals after two rounds of division. Thus, a Pn.p cell was occasionally observed to give rise to four daughter cells without the nuclear envelope ever forming in Pn.pa or Pn.pp. Some, but not all, of these Pn.pxx cells undergo a third round of division, some enter M phase but fail to give rise to daughter cells, and yet others apparently do not divide at all, because they never entered M phase. The abnormal divisions observed in *emb-30(tn475)* homozygotes have made it impossible to determine completely the vulval lineages with certainty. For example, we could not be certain which cells are descended from a particular VPC, and hence how many cells a given VPC generates. Nevertheless, these observations are consistent with the hypothesis that vulval cell divisions exhibit an M-phase defect. It is possible that when the maternally provided *emb-30* gene product be-

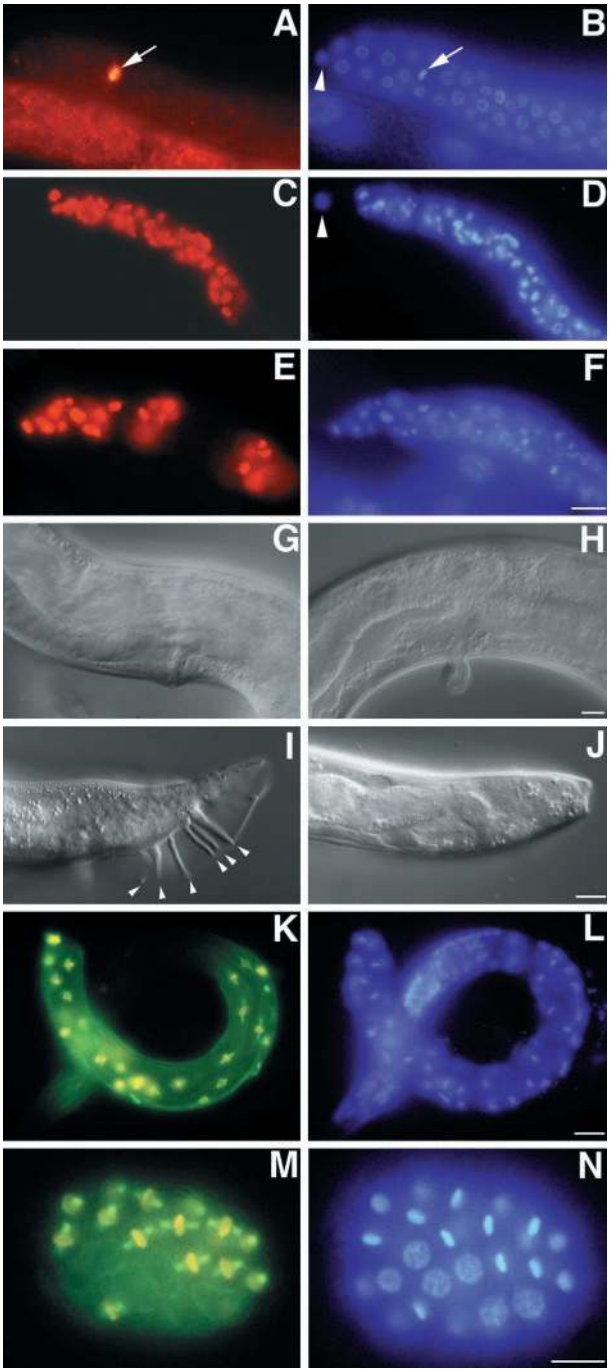

Figure 5. Germline and somatic phenotypes in *emb-30* mutants. L4-stage gonads stained for phosphohistone H3 (A, C, and E) and DNA (B, D, and F). (A and B) Wild-type gonad. A single mitotic germ cell is observed in the distal arm (arrow; arrowhead indicates a distal tip cell). Mitotic germ cells accumulate in *unc-32(e189)emb-30(tn475)* (C and D) and *emb-30(tn475); unc-46(e177)mdf-1(gk2)* (E and F) gonads [*mdf-1(gk2)* homozygotes do not accumulate mitotic cells (Kitagawa and Rose, 1999)]. (G–I) Somatic defects in *emb-30(tn475)* homozygotes. (G) Normal vulva of a rescued *unc-32(e189)emb-30(tn475); tnEx12(F54C8)* adult. (H) Abnormal vulva of an *unc-32(e189)emb-30(tn475)* adult. (I) Wild-type male tail with sensory rays (arrowheads). (J) *unc-32(e189)emb-30(tn475)* male tail; sensory rays are absent. (K–N) Metaphase arrest in *emb-30(m_{ts}, z-)* animals. (K and M) Merged images of tubulin (green) and phosphohistone H3 (red) staining. (L and N) DAPI staining. (K and L) Arrested *emb-30(m_{ts}, z-)* larva with many metaphase cells 24 h after transfer to 25°C. Note the absence of anaphase figures. (M and N) Forty-cell *emb-30(m_{ts}, z-)* embryo containing 23 metaphase cells 2 h after transfer to 25°C from 20°C. Note the absence of anaphase figures. Panels A–F, G and H, I–L, and M and N are at the same scales. Bars, 10 μm.

comes limiting, M phase is lengthened or blocked. The abnormal divisions observed could be related to the occasional observation of three or four centrosomes in mitotic cells (see below).

Thus, *emb-30(class I)* alleles affect multiple postembryonic somatic cell lineages. Moreover, the defects observed are consistent with a defect in cell division rather than in differentiation. Other mutations with widespread postembryonic cell division defects exhibit a sterile-and-uncoordinated phenotype resulting from cell division failures that disrupt ventral nerve cord formation (Albertson *et al.*, 1978; O'Connell *et al.*, 1998). In contrast, *emb-30(class I)* alleles do not display an uncoordinated phenotype. A likely explanation for this difference is that maternally contributed *emb-30* may be sufficient for completion of early larval-stage cell divisions (see below).

Several lines of evidence suggest that class I alleles result from a severe reduction in *emb-30* function: 1) they are the strongest nonconditional *emb-30* alleles; 2) they display a sterile phenotype when placed in trans to a deficiency; 3) they were recovered in unbiased genetic screens at the EMS-knockout frequency (6×10^{-4}); and 4) they result from molecular lesions that are likely to significantly reduce or eliminate gene function (see below).

emb-30 Is Required for the Metaphase-to-Anaphase Transition in Most, if Not All, Cells

Despite the fact that class I alleles severely affect *emb-30* function, many embryonic and larval cell divisions occur normally. One possibility is that *emb-30* is required for some divisions but not others. Alternatively, wild-type maternal *emb-30* function may contribute significantly to the development of class I homozygotes, enabling them to grow into sterile adults. To better address this possibility, we analyzed the development of class I homozygotes under conditions in which maternal *emb-30* function was crippled. To achieve this, we allowed *emb-30(class I)/emb-30(tn377*ts*)* heterozygous animals to lay eggs at a permissive (16°C) or a semipermissive (20°C) temperature and then transferred the gastrula-stage eggs to 25°C (see MATERIALS AND METHODS). The resulting *emb-30(class I)* homozygotes exhibited an embryonic/larval-lethal phenotype, suggesting that the maternal EMB-30^{tn377ts} protein contributed to the *emb-30(class I)* homozygotes [referred to as *emb-30(m_{ts}, z-)* animals for convenience] was less active than the wild type. Staining with anti-phosphohistone H3 and anti-tubulin antibodies suggested that this lethal phenotype was associated with a widespread failure of cells to undergo the metaphase-to-anaphase transition. Many somatic cells arrested in metaphase with normal spindles (Figure 5, K and L). Moreover,

the terminal-stage embryos arrested with many mitotic cells (Figure 5, M and N). To quantitate this widespread mitotic arrest, we defined the Worm Mitotic Index (WMI) as the population average of the number of mitotic nuclei in L1- or L2-stage animals. We found the WMI of *emb-30(m_{ts}, z-)* animals to be 26.5 ± 13 (n = 39), significantly different from the wild-type WMI value of 1.6 ± 2.8 (n = 39). We also observed that 18% of the mitotically arrested cells scored (n = 164) contained three or four centrosomes, suggesting a limited capacity of the centrosomes to divide in the absence of anaphase and mitotic exit. In contrast, we observed only two centrosomes in mitotic cells (n = 61) in the wild type. Based on these results, we conclude that: 1) *emb-30* is likely to be required for most, if not all, metaphase-to-anaphase transitions; 2) maternally encoded *emb-30* product contributes to the development of *emb-30(class I)* homozygotes; and 3) *emb-30(tn377*ts*)* must also affect somatic functions in a dosage-sensitive manner such that the germ line is more sensitive than the soma.

Mitotic Arrest in emb-30 Mutants Occurs in the Absence of the Spindle Assembly Checkpoint

Studies from other systems have established that antimicrotubule agents, e.g., nocodazole, can block the metaphase-to-anaphase transition (Gaulden and Carlson, 1951; Sluder, 1979) by activating the spindle assembly checkpoint (Hoyt *et al.*, 1991; Li and Murray, 1991). Both subtle alterations, such as single improperly oriented chromosomes (Callan and Jacobs, 1957; Rieder *et al.*, 1994; Li and Nicklas, 1995), and more drastic perturbations of spindle or kinetochore components (Yen *et al.*, 1991; Hardwick *et al.*, 1999) can activate the spindle assembly checkpoint. Thus, the metaphase-to-anaphase transition defects observed in *emb-30* mutants could, in principle, result from checkpoint activation as a secondary consequence of the mutant defect. Alternatively, *emb-30* could be an essential requirement for the metaphase-to-anaphase transition even in the absence of the checkpoint. To choose between these two possibilities, we conducted a genetic epistasis test with a null allele in *mdf-1*, the putative *C. elegans* orthologue of the MAD1 gene (Kitagawa and Rose, 1999). *mdf-1* has been shown to be required for mitotic cell cycle arrest in the distal arm of the gonad in response to nocodazole (Kitagawa and Rose, 1999). We analyzed the distal mitotic zone of the gonad in *unc-46(e177) mdf-1(gk2); emb-30(tn475)* double mutants at the L4 and adult stages and found that mitotic nuclei accumulate as in *emb-30(tn475)* single mutants (Figure 5, A–F; our unpublished results). This genetic test indicates that the metaphase-to-anaphase transition defects in *emb-30(class I)* mutants are not due to activation of the spindle assembly checkpoint.

The spindle assembly checkpoint mechanism is essential in *C. elegans*: an *mdf-1* null mutation causes a highly penetrant maternal-effect lethal/sterile phenotype that is likely to result from chromosome missegregation during mitosis (Kitagawa and Rose, 1999). We reasoned that a reduction in *emb-30* function might be able to suppress *mdf-1* mutant phenotypes by delaying the metaphase-to-anaphase transition. According to this hypothesis, a delay in the metaphase-to-anaphase transition might partially compensate for the absence of the "wait" signal generated by the spindle assembly checkpoint mechanism. To test this hypothesis, we compared the viability and fertility of *unc-46(e177) mdf-1(gk2); emb-30(tn377*ts*)* homozygotes with *unc-46(e177) mdf-1(gk2)* homozygotes at 16°C (Table 4). *unc-46(e177) mdf-1(gk2)* homozygotes cannot be maintained as a homozygous culture because of a high degree of embryonic/larval arrest and sterility (Table 4). In contrast, *unc-46(e177) mdf-1(gk2); emb-30(tn377*ts*)* homozygotes grow well and can be maintained as a homozygous culture at 16°C (Table 4). Strikingly, *emb-30(tn377*ts*)* can partially suppress most *mdf-1* mutant phenotypes at 16°C. For example, whereas most *mdf-1* homozygotes arrest as embryos or larvae, most *mdf-1; emb-30(tn377*ts*)* double mutants survive to adulthood (Table 4). Furthermore, whereas only a small fraction of *mdf-1* homozygotes have a brood size (total number of eggs produced by a single hermaphrodite) > 10, a substantial proportion of *mdf-1; emb-30(tn377*ts*)* double mutants have a brood size > 10 (Table 4). The slight increases in adult sterility and in the L2–L4-arrest phenotype (Table 4) may reflect incomplete suppression, with some embryos and L1 larvae arresting at a later stage in the double mutant. Together, these genetic results show that reducing *emb-30* activity can substantially suppress the lethality and sterility caused by a defect in the spindle assembly checkpoint mechanism. Based on these results, we suggest that delaying the onset of anaphase can bypass the requirement of spindle checkpoint function for normal development.

Table 4. Partial suppression of *mdf-1(gk2)* mutant phenotypes by *emb-30(tn377*ts*)*

	Parental genotype[a]	
Phenotype[b]	*mdf-1(gk2)* (n = 813)	*emb-30(tn377*ts*); mdf-1(gk2)* (n = 1740)
Embryonic arrest	22.5%	12.6%
L1 arrest	57.8%	11.0%
L2–L4 arrest	4.9%	6.4%
Sterile adult	13.5%	19.7%
Male	1.8%	0.5%
Brood size[c] = 1–10	0.7%	5.4%
Brood size[c] = 11–50	0.1%	14.5%
Brood size[c] = 51–100	0.1%	17.1%
Brood size[c] = > 100	0%	12.9%

[a] The complete broods of 6 *unc-46(e177) mdf-1(gk2)* and 10 *emb-30(tn377*ts*); unc-46(e177) mdf-1(gk2)* homozygotes were analyzed at 16°C. These parental animals were the F1 progeny of *+/eT1III; unc-46(e177) mdf-1(gk2)/eT1V* and *emb-30(tn377*ts*)/eT1III; unc-46(e177) mdf-1(gk2)/eT1V* heterozygotes, respectively.

[b] Phenotypes were scored as described (Kitagawa and Rose, 1999).

[c] Brood size refers to the total number of eggs produced by a single adult hermaphrodite.

emb-30 Encodes an APC4 Homologue and Contains WD Repeats Divergently Related to Cdc20 Family Proteins

Using genetic and physical markers, we mapped *emb-30* to the ~140-kb *emb-9–sod-4* interval on chromosome III (Figure 6A; Table 5). PCR and Southern blot hybridization experi-

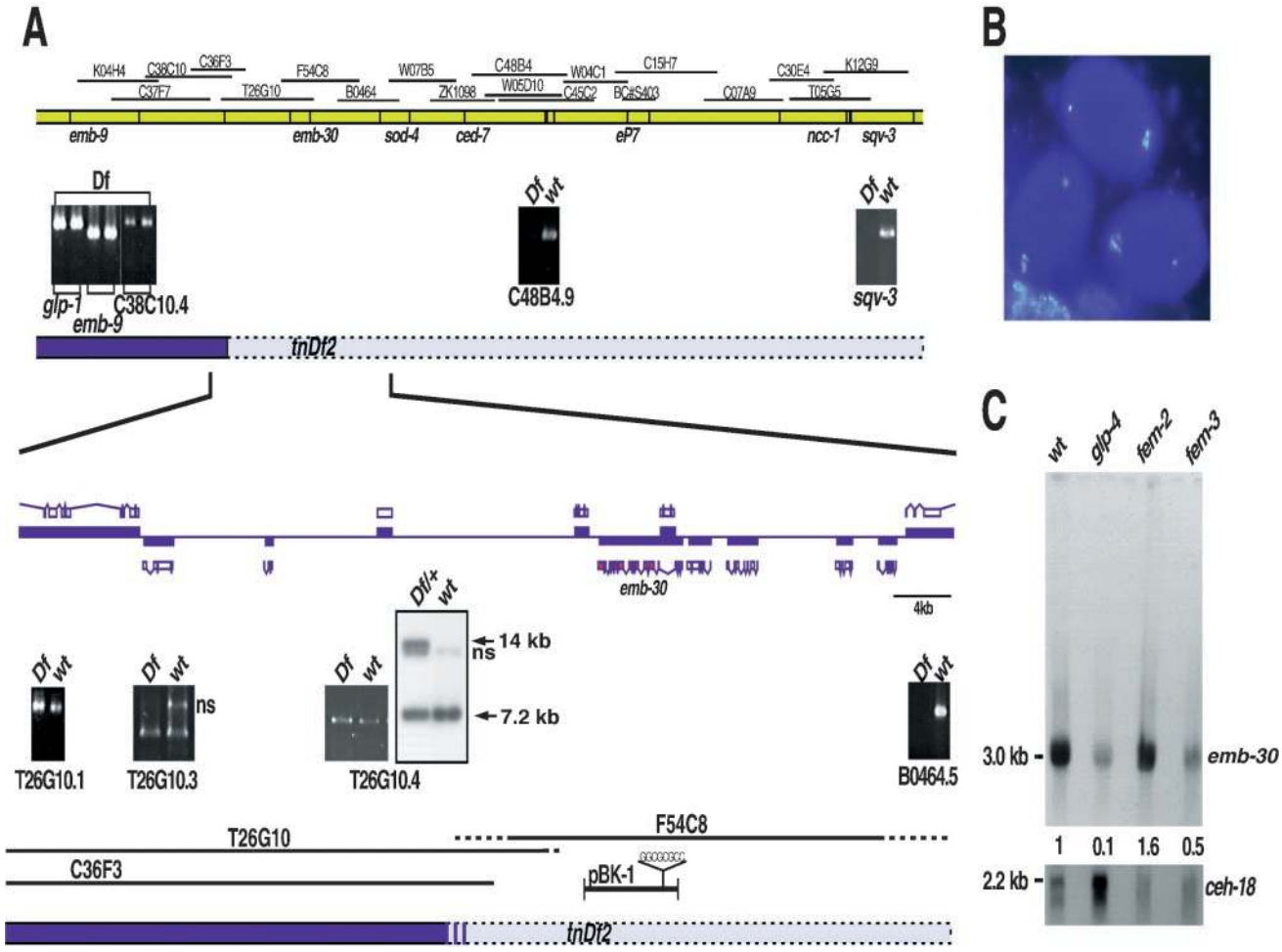

Figure 6. Molecular identification of *emb-30*. (A) Genetic and physical map of the *emb-30III* region. (Top) Sequenced cosmids. Sequence tag site analysis (panels with black background) positioned the *tnDf2* left breakpoint between C38C10.4 and C48B4.9. (Bottom) Enlarged physical map. ORFs are shown above and below the line, with their directions of transcription being left to right and right to left, respectively. The *sod-4* ORF is not shown but would be to the right. Predicted genes from cosmid T26G10 are not deleted, whereas B0464.5 is deleted. The *tnDf2* left breakpoint was detected by Southern hybridization with the use of a T26G10.4 probe. A novel 14-kb band is detected in *tnDf2*/+ heterozygotes (wild-type band, 7.2 kb; ns, nonspecific band). (B) Identification of *emb-30* with the use of RNAi. DAPI-stained embryos resulting from injection of F54C8.3 double-stranded RNA (exons 2–15) arrest at the one-cell stage and do not form polar bodies (*emb-30* mutant phenocopy). (C) *emb-30* is expressed in the germ line and the soma. Northern hybridization to young-adult-stage poly(A)+ RNA from germline developmental mutants: *glp-4(bn2*ts*)*, no germ line; *fem-2(b245*ts*)*, oocytes only; and *fem-3(q20* gf, ts*)*, sperm only.

ments localized the left breakpoint of *tnDf2* ~ 1.5 kb to the right of the predicted gene T26G10.4 (Figure 6A). We then applied RNAi to predicted genes located right of the *tnDf2* breakpoint to identify *emb-30*. RNAi targeted to the predicted gene, F54C8.3, phenocopied the *emb-30* one-cell-arrest mutant phenotype: RNAi embryos arrested at the one-cell stage (99%; n = 78) and did not form pronuclei or polar bodies (Figure 6B). Moreover, cosmid F54C8 and a 10-kb clone containing F54C8.3, pBK1 (see Figure 6A), rescued the vulval defect of *emb-30(tn475)* mutants in one of five and three of five stable lines, respectively (Figures 5G and 6A; our unpublished results). In a few instances, we observed that rescued *emb-30(tn475)* homozygotes laid a few eggs, which arrested during embryogenesis, suggesting weak rescue of germline phenotypes. A predicted gene, F54C8.1, with similarity to 3-hydroxyacl–coenzyme A dehydrogenase, is located within *emb-30* intron 3 (see below and Figure 6A) and encoded by the opposite strand. The rescuing subclone, pBK1, contained an introduced N-terminal frameshift in F54C8.1, allowing us to discount the hypothesis that F54C8.1 was involved in *emb-30* function in any way (Figure 6A). DNA sequence analysis of the 16 chemically generated *emb-30* mutant alleles provided further confirmation that *emb-30* corresponds to F54C8.3 (Figure 7).

The *C. elegans* Expressed Sequence Tag project had identified 14 cDNA clones corresponding to F54C8.3 (Y. Kohara, personal communication). Five overlapping cDNA clones (yk240d9, yk317d3, yk180e2, yk378b2, and yk133f2) were used as probes in Northern blot hybridization of poly(A)+ RNA and detected a single 3.0-kb transcript (Figure 6C; our

Table 5. Physical and genetic mapping of *emb-30*

Parental genotype	Recombinant phenotype	Genotype of recombinant chromosome[a]	Number
*sma-2(e502) emb-30(tn377*ts*) ced-7(n1892) unc-69(e587)/sod-4(pk68::Tc1)*[b]	Sma non-Unc	*sma-2(e502) sod-4(pk68::Tc1)*	21/77
		*sma-2(e502) emb-30(tn377*ts*) sod-4(pk68::Tc1)*	5/77
		*sma-2(e502) emb-30(tn377*ts*)*	3/77
		*sma-2(e502) emb-30(tn377*ts*) ced-7(n1892)*	48/77
	Non-Sma Unc	*emb-30(tn377*ts*) ced-7(n1892) unc-69(e587)*	38/124
		ced-7(n1892) unc-69(e587)	3/124
		sod-4(pk68::Tc1) ced-7(n1892) unc-69(e587)	3/124
		sod-4(pk68::Tc1) unc-69(e587)	80/124
emb-9(hc70 sd, ts*) unc-69(e587)/unc-36(e251) emb-30(tn377*ts*)*[c]	Non-Emb-9 Unc-69	*unc-36(e251) unc-69(e587)*	4/82
		*unc-36(e251) emb-30(tn377*ts*) unc-69(e587)*	78/82
emb-9(hc70 sd, ts*) unc-69(e587)/emb-30(tn471)*[d]	Non-Emb-9 Unc-69	*unc-69(e587)*	3/55
		emb-30(tn471) unc-69(e587)	52/55

[a] Genes are listed in left-to-right order on *LGIII*. *unc-36*, *sma-2*, and *unc-69* are not shown in Figure 6.

[b] The presence of *sod-4(pk68::Tc1)* was scored by PCR (see MATERIALS AND METHODS).

[c] Recombinants were picked at 25°C and placed at 15°C.

[d] Recombinants were picked at 22.5°C.

unpublished results). DNA sequence analysis of the cDNA clones suggested that yk240d9 was likely to correspond to a full-length *emb-30* transcript because it contained 5 bp of the SL2 *trans*-spliced leader sequence at the 5′ end and poly(A) residues at the 3′ end. RT-PCR analysis suggested that *emb-30* could be both SL1 and SL2 *trans* spliced with the use of a single acceptor sequence (Figure 7; our unpublished results). This SL1/SL2 splice-acceptor sequence is required for *emb-30* function, because *tn472* results from a G-to-A change in the conserved TTTCAG acceptor sequence and causes a strong loss of function (Figure 7). Northern blot comparison of the wild type with *glp-4(bn2*ts*)* mutants, which produce ~12 germ cells (Beanan and Strome, 1992), indicated that the *emb-30* transcript is ~10-fold more abundant in adults that produce a germ line (Figure 6C). The *emb-30* transcript is enriched (~3-fold) when the germ line is specified in the female mode of development in *fem-2(b245*ts*)* mutants compared with a masculinized germ line [*fem-3(q20*gf*)*].

DNA sequence analysis of the full-length cDNA clone (yk240d9) and three partial clones (yk180e2, yk317d3, and yk80d6) indicated that *emb-30* has 15 exons and 14 introns and spans 6 kb of genomic sequence (Figure 7). Consistent with the Northern blot data, we found no evidence for alternative splicing or use of alternative 5′ ends. Slight variation in 3′ untranslated region length was observed: five cDNA clones had their 3′ ends within 160 bp after the stop codon, whereas yk317d3 had its 3′ end ~405 bp after the

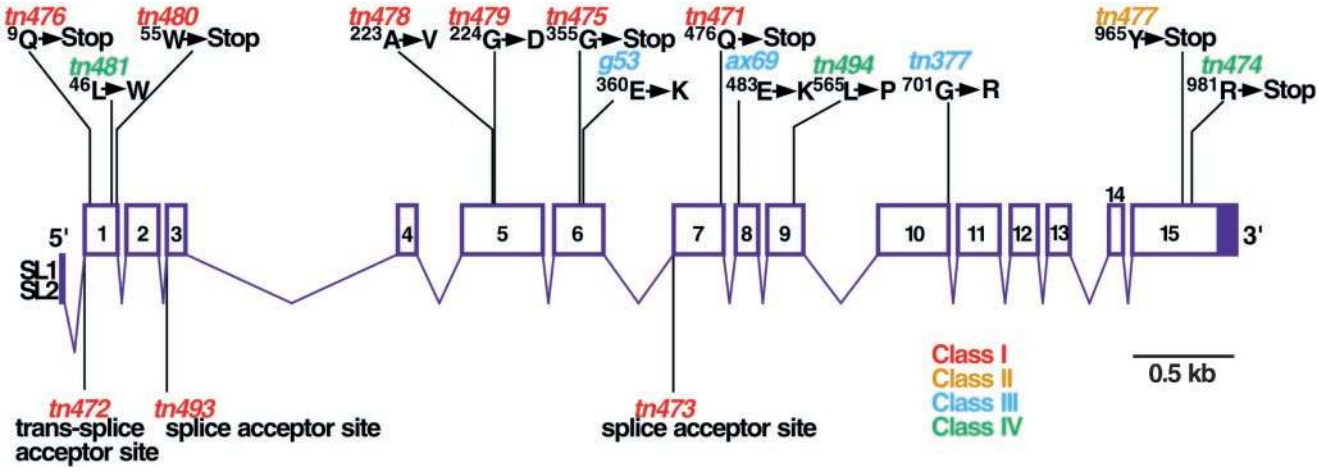

Figure 7. Molecular and genomic structure of *emb-30*. Exons are represented by numbered boxes, with filled regions indicating noncoding sequences. *emb-30* mutant alleles are indicated.

stop codon. Using a yk317d3 3′ end–specific probe, we were unable to detect a transcript upon Northern blot analysis of mixed-stage poly(A)+ RNA (our unpublished results). Therefore, the yk317d3 cDNA clone is likely to represent a minor mRNA.

Conceptual translation of the *emb-30* cDNA indicates that *emb-30* could encode a 1027-amino acid protein, EMB-30, with a predicted molecular mass of 117 kDa (Figures 7 and 8). The first methionine is likely to be the translation initiator because *tn476* introduces a stop codon at position 9 (Figure 7) and results in a strong loss of function (the next methionine residue is at position 26). Based on amino acid composition, EMB-30 is predicted to be a highly charged acidic hydrophilic protein with a predicted isoelectric point of 4.7 (17% glutamic acid and aspartic acid residues, 11% lysine and arginine residues).

BLAST searches revealed that EMB-30 shares amino acid sequence similarity with human APC4 (hAPC4), a biochemically characterized component of the APC/C (Yu e*t al.*, 1998). Both EMB-30 and hAPC4 also exhibit similarly to *S. pombe* Lid1, a genetically and biochemically characterized component of the APC/C (Berry *et al.*, 1999; Yamashita *et al.*, 1999), as revealed by BLAST searches with hAPC4. Amino acid sequence alignments with the use of CLUSTAL W indicated that EMB-30, hAPC4, and Lid1 could be aligned along their entire lengths with the introduction of several gaps (Figure 8). In this alignment, EMB-30 shares 16% identity and 29% similarity with hAPC4 and 13% identity and 26% similarity with Lid1. This level of amino acid sequence similarity is comparable to that shared by hAPC4 and Lid1, which are 18% identical and 33% similar. In contrast, *S. cerevisiae* APC4 is more highly divergent, consistent with the suggestion that APC4 may represent an APC component that has diverged more during evolution than other subunits (Zachariae *et al.*, 1998; our unpublished results). Based on these results and the *emb-30* mutant phenotype, we conclude that EMB-30 is the likely *C. elegans* APC4 orthologue.

Previously, no known motifs were recognized in APC4 family proteins (Yu *et al.*, 1998; Zachariae *et al.*, 1998; Berry *et al.*, 1999; Yamashita *et al.*, 1999). However, BLAST searches revealed that the EMB-30 N-terminal region was related to WD repeats (Neer *et al.*, 1994). Multiple sequence alignments further showed the presence of six contiguous WD repeats divergently related to WD repeats found in Cdc20 family proteins, as indicated by the presence of highly conserved amino acid residues (Figure 9). Cdc20 proteins and the related Hct1p have seven WD repeats and are thought to function as substrate-specific activators of the APC/C (reviewed by Zachariae and Nasmyth, 1999). WD repeats 1–5 of EMB-30 (WD1–WD5) are most related to repeats WD3–WD7 of the Cdc20 proteins, respectively (Figure 9). EMB-30 WD1 and WD2 are the most highly conserved repeats compared with the Cdc20 family members. WD1 and WD2 of EMB-30 share 28 and 20% amino acid identity with WD3 and WD4 from *S. cerevisiae* Cdc20, respectively. In contrast, EMB-30 WD6 is highly divergent but is most closely related to EMB-30 WD2. WD1 and WD2 are also clearly recognizable in both hAPC4 and Lid1. X-ray crystallographic analysis suggests that WD repeats can form a propeller-like structure, with the four antiparallel β-pleated sheets of a repeat constituting a blade (Wall *et al.*, 1995; Sondek *et al.*, 1996). Structural studies will be required to determine whether the divergent WD repeats we defined in EMB-30 or the APC4 homologues can adopt this conformation.

Three *emb-30* mutant alleles result in single amino acid substitutions within the WD domain (Figures 7–9). The two strongest missense mutations, found in the class I alleles *tn478* and *tn479*, result in amino acid changes (A223V and G224D, respectively) in WD5. These amino acids are not shared with hAPC4 or Lid1 (Figure 8). The viable weak allele, *tn481*, results in an amino acid substitution (L46W) at a position conserved in hAPC4 (Figure 8). This position is also adjacent to a highly conserved residue (I44) in WD1 (Figure 9). However, the positions of missense mutations and the placement of nonsense mutations also suggest that the WD repeats of EMB-30 are unlikely to be sufficient for function. The four missense mutations in the *emb-30* alleles, *g53*ts, *ax69*ts, *tn494*, and *tn377*ts, all lie C terminal to the WD repeats (Figures 7–9). Moreover, nonsense mutations caused by the class I alleles *tn471* and *tn475* are predicted to truncate the protein C terminal to the WD repeats (Figures 7 and 9). Because both *emb-30(tn471)* and *emb-30(tn475)* are not suppressible by *smg* mutations, which interfere with nonsense-mediated RNA decay, truncated products encoded by the mutant alleles are unlikely to function normally.

The EMB-30 C Terminus Is Specifically Required for Completion of the Oocyte Meiotic Divisions

A single recessive allele, *emb-30(tn477)*, defines phenotypic class II and results in a completely penetrant nonconditional strict maternal-effect lethal phenotype (Table 3). Analysis of the origin of the maternal-effect lethality indicates that *emb-30(tn477)* is defective in completion of the oocyte meiotic divisions and results in a one-cell-arrest phenotype. In contrast, spermatocytes in *emb-30(tn477)* appear normal and are able to complete both meiotic divisions, producing sperm that appear normal and that can fertilize *emb-30(tn477)* oocytes. *emb-30(tn477)* hermaphrodites and males have no apparent somatic defects. The vulval cell lineages were analyzed in seven *unc-32(e189)emb-30(tn477)* animals and were found to be completely normal. There was no evidence for delays in divisions or lengthening of mitosis. Heterozygous *emb-30(tn477)/emb-30(tn475)* hermaphrodites were constructed (n = 16; *tn475* is a class I allele) and found to have a Mel phenotype. Similarly, *emb-30(tn477)* fails to complement *emb-30(tn377*ts*)* for the Mel phenotype but complements for the Glp phenotype. Thus, *emb-30(tn477)* results in a very specific defect in the ability of oocytes to complete the meiotic divisions after fertilization. Likewise, a viable class IV allele, *tn474*, fails to complement *emb-30(tn377*ts*)* for the Mel phenotype but also complements for the Glp phenotype: all *emb-30(tn474)/emb-30(tn377*ts*)* hermaphrodites produce embryos that arrest at the one-cell stage, failing to complete the meiotic divisions at 25°C (n > 1000). Importantly, both *emb-30(tn477)* and *emb-30(tn474)* are *smg* suppressible: *smg-1(r861); emb-30(tn477)* and *smg-1(r861); emb-30(tn474)/emb-30(tn377*ts*)* hermaphrodites are fertile. Both *tn477* and *tn474* result from nonsense mutations that are predicted to cause C-terminal truncations, removing 63 and 46 amino acids, respectively (Figure 7). The *smg* system is required for nonsense-mediated mRNA decay (Anderson and Kimble, 1997); thus, suppression is likely to result from the increased production of the truncated products. Based on these genetic results, we propose that the EMB-30 C

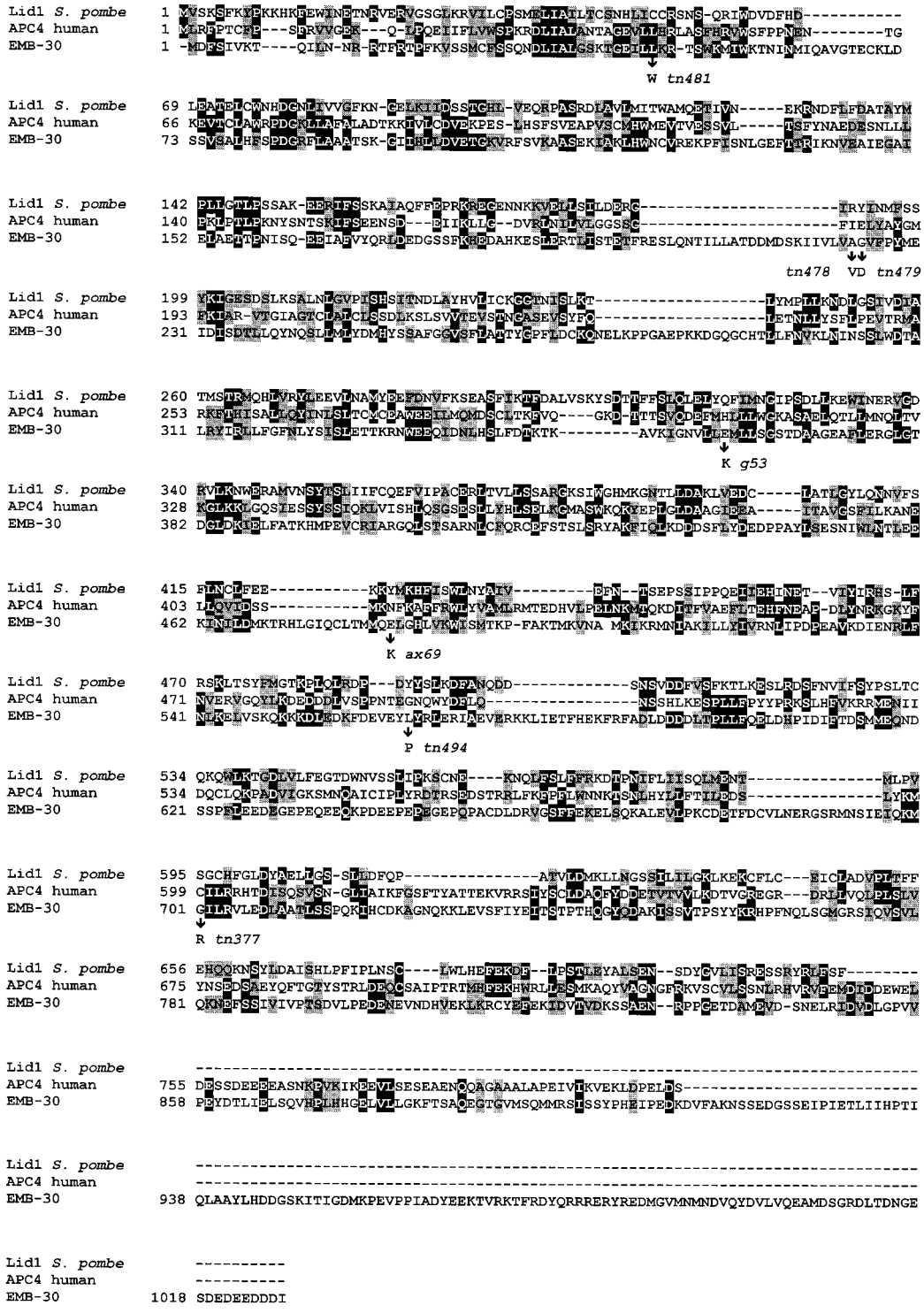

Figure 8. Amino acid sequence alignment of EMB-30 with *S. pombe* Lid1 and human APC4. Amino acid identities and similarities are represented by black and gray boxes, respectively. The positions of *emb-30* missense mutations are indicated. GenBank accession numbers: EMB-30, AF192400; human APC4, AF191338; and Lid1, AB025243.

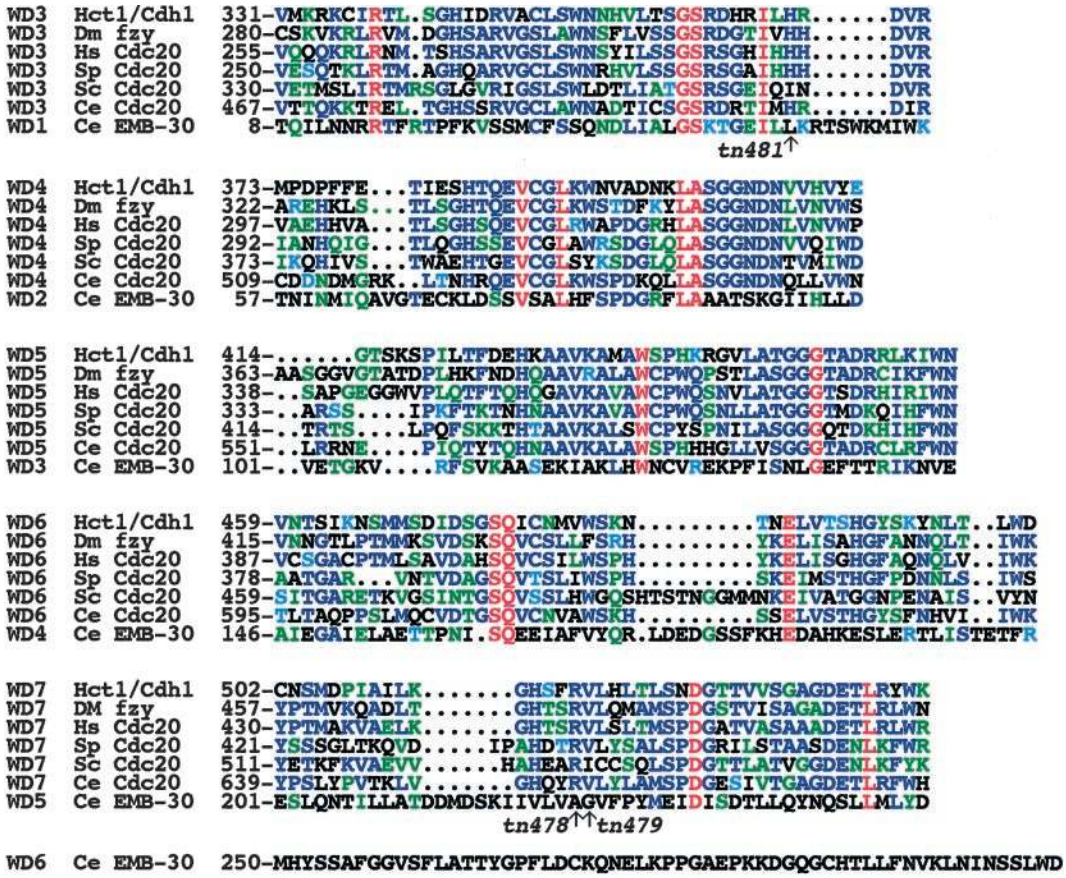

Figure 9. Amino acid sequence alignment of EMB-30 WD1–WD5 with WD3–WD7 from Cdc20 family members. Conserved residues are shown in colors: red, identical in all; blue, conserved in at least three; and green, conserved in two. Cyan represents the chemical similarity of arginine to lysine and threonine to serine. EMB-30 WD2 is the most conserved repeat. The positions of *emb-30* mutant alleles in the WD domain are indicated with arrows. GenBank accession numbers: *S. cerevisiae* (Sc) Hct1/Cdh1, Z72525; *Drosophila melanogaster* (Dm) fzy, AAA83150; *Homo sapiens* (Hs) Cdc20 (p55CDC), U05340; *S. pombe* (Sp) Cdc20, AAC49621; *S. cerevisiae* (Sc) Cdc20, P26309; and putative *C. elegans* (Ce) Cdc20 (predicted gene ZK1307.6), CAA87433.

terminus is required for normal protein stability in the oocyte. One possibility is that the C-terminal deletions destabilize EMB-30 only in the oocyte. Alternatively, the C-terminal deletions may destabilize EMB-30 in all tissues, but the oocyte meiotic divisions may be the most sensitive to this partial loss of *emb-30* function.

DISCUSSION

The metaphase-to-anaphase transition is a critical juncture in the eukaryotic cell cycle. The metaphase-to-anaphase transition and mitotic exit are regulated by the APC/C that catalyzes the ubiquitination of anaphase inhibitors (e.g., Pds1p) and mitotic cyclins, thereby targeting them for degradation by the proteasome (reviewed by Zachariae and Nasmyth, 1999). We show here that *emb-30* is required for the transition from metaphase to anaphase during meiosis and mitosis in *C. elegans*. Mitotic arrest in *emb-30* mutants occurs even in the absence of the spindle assembly checkpoint mechanism that regulates entry into anaphase. We have cloned *emb-30* and shown that it encodes the likely *C. elegans* orthologue of Lid1/APC4, a component of the APC/C (Yu *et al.*, 1998; Zachariae *et al.*, 1998; Berry *et al.*, 1999; Yamashita *et al.*, 1999). Thus, our results provide direct in vivo evidence that EMB-30, and by inference the APC/C, is likely to be required for all metaphase-to-anaphase transitions in a multicellular organism. Importantly, all *emb-30* mutant phenotypes observed are likely to be the direct consequence of metaphase-to-anaphase transition defects, suggesting that this is the only essential *emb-30* function.

C. elegans oocytes lacking *emb-30* activity undergo nuclear envelope breakdown, ovulation, and fertilization identical to the wild type. Morphologically normal spindles are formed after fertilization, and condensed bivalents are visible on the metaphase plate. Thus, progression to metaphase of the first meiotic cell cycle is apparently normal in the absence of *emb-30*. In the wild type, fertilized embryos progress rapidly through MI and MII, producing two polar bodies. Upon completion of MII, the maternal and paternal pronuclei form. Shortly thereafter, the pronuclei fuse as the zygote enters the first mitotic cell cycle. In contrast, in *emb-30* mutants, fertilized oocytes fail to progress to anaphase I: chro-

mosome segregation fails to occur, polar bodies are not produced, and pronuclei never form. *emb-30* mutant embryos fail to undergo cytokinesis and arrest at the one-cell stage. The failure of *emb-30* mutant embryos to form pronuclei is consistent with a requirement of the APC/C for M-phase exit.

Our results indicate that the defect we observe in *emb-30* mutants is in cell cycle progression and does not reflect a failure of fertilization to occur properly. Specifically, we have shown that mutations in *emb-30* can block the endomitotic cell cycle that occurs in unfertilized oocytes. In addition, we have shown that *emb-30* is also required for meiosis to occur properly in spermatocytes. Primary spermatocytes lacking *emb-30* activity are unable to complete the meiotic divisions, residual bodies do not form, and sperm are not produced.

Our analysis indicates that in addition to its role in the metaphase-to-anaphase transition during meiosis, *emb-30* is also required for many, and perhaps all, mitotic divisions during the development of both the germ line and the soma. Embryos or larvae of genotype *emb-30*(m_{ts}, *z-)* (i.e., those containing maternally derived protein encoded by the ts allele *tn377*ts and homozygous for a class I severe-reduction-of-function *emb-30* allele) arrest development when shifted to the restrictive temperature, with many somatic cells apparently blocked at the metaphase-to-anaphase transition. Temperature-shifted *emb-30(tn377*ts*)* hermaphrodites and males show a strong germline proliferation defect that results from a failure of mitosis in the germline precursor cells Z2 and Z3; these cells block in mitosis of their first cell division. As in *emb-30* mutant oocytes, nuclear envelope breakdown occurs and the metaphase plate forms. However, the cells do not progress further. Anaphase and cytokinesis both fail to occur, and the nuclear envelope does not reform. Analysis of the distal mitotic zone of the adult hermaphrodite gonad suggests that *emb-30* is continually required for germline mitosis.

Anaphase onset is regulated by the spindle assembly checkpoint (reviewed by Amon, 1999). Recently, it has been shown that Cdc20p is a direct target of the spindle assembly checkpoint (Hwang *et al.*, 1998; Kim *et al.*, 1998). A model has been proposed in which the spindle assembly checkpoint mechanism senses the presence of unattached kinetochores and directly inhibits Cdc20p, thus preventing activation of the APC/C (reviewed by Amon, 1999). Consistent with this model, genetic epistasis analysis indicates that *emb-30* mitotic arrest occurs in the absence of the spindle checkpoint. Nocodazole treatment causes mitotic cells in the distal arm of the gonad to block in mitosis. A putative *C. elegans* homologue of the MAD1 gene, *mdf-1*, has been shown to be required for mitotic arrest in response to nocodazole (Kitagawa and Rose, 1999). In *emb-30*; *mdf-1* double mutants, however, mitotic germ cells are also blocked in mitosis, suggesting that this block is not a secondary consequence of spindle checkpoint activation but rather reflects an essential requirement for *emb-30* function. Strikingly, a reduction in *emb-30* function substantially suppresses *mdf-1* mutant phenotypes that are likely to arise from a spindle assembly checkpoint defect. These suppression data suggest that delaying the onset of anaphase can bypass the requirement for the spindle assembly checkpoint for normal development. Moreover, this result provides experimental support for the idea that the primary essential role for the spindle checkpoint is in regulating anaphase onset rather than in the chromosome segregation process per se.

Several observations suggest that the spindle assembly checkpoint does not function during oocyte meiotic maturation. Nocodazole treatment of *C. elegans* oocytes before fertilization blocks the production of polar bodies but not the formation of pronuclei (T. Doniach, personal communication). Furthermore, embryos harboring mutations in *mei-1*, *mei-2*, or *zyg-9*, which encode components of the oocyte spindle, are not blocked at metaphase, even though the meiotic spindle is severely abnormal and DNA segregation is defective (Clark-Maguire and Mains, 1994; Matthews *et al.*, 1998). The fact that *emb-30* mutant embryos arrest at metaphase, therefore, suggests that *emb-30* is required for some other aspect of the progression to anaphase (or exit from metaphase).

APC/C activation at anaphase requires the function of Cdc20p, a member of a conserved family of WD-repeat proteins that binds the APC/C. In *Drosophila*, mutations in *fizzy*, a CDC20 orthologue, block the degradation of cyclins A and B and arrest the embryonic cell cycle in metaphase (Dawson *et al.*, 1995; Sigrist *et al.*, 1995). Current data have led to the model that Cdc20 family members are substrate-specific activators of the APC/C; Cdc20p preferentially targets Pds1p for destruction, whereas the related Hct1p/Cdh1p targets ubiquitination of cyclin B. Because EMB-30 contains WD repeats that are divergently related to those found in Cdc20 family members, there appears to be an evolutionary relationship between an APC/C component and APC/C activators. Because WD repeats often mediate protein–protein interactions (Neer *et al.*, 1994), it is tempting to speculate that Cdc20p and EMB-30/Lid1/APC4 bind APC/C components via the WD repeats.

ACKNOWLEDGMENTS

The authors are grateful to Kathy Gould, David Miller, Gary Ruvkun, Lilliana Solnica-Krezel, and Chris Wright for helpful discussions, comments on the manuscript, and encouragement. Tabitha Doniach and Tim Schedl generously communicated unpublished data. Beth DeStasio and Lois Edgar kindly provided advice on ENU and TMP mutagenesis, respectively. We thank Yuji Kohara for cDNA clones, Alan Coulson for cosmids, and Susan Strome for antibodies. Andy Golden, Tim Schedl, Heinke and Ralf Schnabel, and Liz Speliotes provided useful strains and suggestions. Two anonymous reviewers provided helpful comments on the manuscript. We thank Kolari Bhatt for DNA sequencing performed at the Vanderbilt-Ingram Cancer Center sequencing core facility, funded by Cancer Center Support grant 1P30 CA68485. This work was supported by grants from the American Cancer Society (DB-149 and JFRA-630) and the National Institutes of Health (GM57173). Some strains used in this study were provided by the *Caenorhabditis* Genetics Center, which is supported by the National Institutes of Health's National Center for Research Resources.

REFERENCES

Albertson, D.G. (1984). Formation of the first cleavage spindle in nematode embryos. Dev. Biol. *101*, 61–72.

Albertson, D.G., Sulston, J.E., and White, J.G. (1978). Cell cycling and DNA replication in a mutant blocked in cell division in the nematode *C. elegans*. Dev. Biol. *63*, 165–178.

Albertson, D.G., and Thomson, J.N. (1993). Segregation of holocentric chromosomes at meiosis in the nematode, *Caenorhabditis elegans*. Chromosome Res. *1*, 15–26.

Altschul, S.F., Madden. T.L., Schäffer, A.A., Zhang. J., Zhang, Z., Miller, W., and Lipman, D.J. (1997). Gapped BLAST and PSI-BLAST: a new generation of protein database search programs. Nucleic Acids Res. *25*, 3389–3402.

Amon, A. (1999). The spindle checkpoint. Curr. Opin. Genet. Dev. *9*, 69–75.

Anderson, P., and Kimble, J. (1997). mRNA and translation. In: *C. elegans* II, ed. D. Riddle, T. Blumenthal, B. Meyer, and J. Preiss, Cold Spring Harbor, NY: Cold Spring Harbor Laboratory, 185–208.

Beanan, M.J., and Strome, S. (1992). Characterization of a germ-line proliferation mutation in *C. elegans*. Development *116*, 755–766.

Berry, L.D., Feoktistova, A., Wright, M.D., and Gould, K.L. (1999). The *Schizosaccharomyces pombe dim1*$^+$ gene interacts with the anaphase-promoting complex or cyclosome (APC/C) component lid1$^+$ and is required for APC/C function. Mol. Cell. Biol. *19*, 2535–2546.

Blose, S.H., Meltzer, D.I., and Feramisco, J.R. (1984). 10-nm filaments are induced to collapse in living cells microinjected with monoclonal and polyclonal antibodies against tubulin. J. Cell Biol. *98*, 847–858.

Boxem, M., Srinivasan, D.G., and van den Heuvel, S. (1999). The *Caenorhabditis elegans* gene *ncc-1* encodes a cdc2-related kinase required for M phase in meiotic and mitotic cell divisions, but not for S phase. Development *126*, 2227–2239.

Brenner, S. (1974). The genetics of *Caenorhabditis elegans*. Genetics *77*, 71–94.

Callan, H.G., and Jacobs, P.A. (1957). The meiotic process in *Mantis religiosa* L. males. J. Genet. *55*, 200–217.

Cassada, R., Isnenghi, E., Culotti, M., and von Ehrenstein, G. (1981). Genetic analysis of temperature-sensitive embryogenesis mutants in *C. elegans*. Dev. Biol. *84*, 193–205.

Clark-Maguire, S., and Mains, P.E. (1994). Localization of the *mei-1* gene product of *Caenorhabditis elegans*, a meiotic-specific spindle component. J. Cell Biol. *126*, 199–209.

Davis, L.I., and Blobel, G. (1986). Identification and characterization of a nuclear pore complex protein. Cell *45*, 699–709.

Dawson, I.A., Roth, S., and Artavanis-Tsakonas, S. (1995). The *Drosophila* cell cycle gene *fizzy* is required for normal degradation of cyclins A and B during mitosis and has homology to the *CDC20* gene of *Saccharomyces cerevisiae*. J. Cell Biol. *129*, 725–737.

Denich, K.T.R., Schierenberg, E., Isnenghi, E., and Cassada, R. (1984). Cell-lineage and developmental defects of temperature-sensitive embryonic arrest mutants of the nematode *C. elegans*. Roux's Arch. Dev. Biol. *193*, 164–179.

DeStasio, E., Lephoto, C., Azuma, L., Holst, C., Stanislaus, D., and Uttam, J. (1997). Characterization of revertants of *unc-93(e1500)* in *Caenorhabditis elegans* induced by N-ethyl-N-nitrosourea. Genetics *147*, 597–608.

Edgar, L.G. (1995). Blastomere culture and analysis. In: Methods in Cell Biology, ed. H. Epstein and D. Shakes, San Diego, CA: Academic Press, 303–421.

Fire, A., Xu, S., Montgomery, M.K., Kostas, S.A., Driver, S.E., and Mello, C.C. (1998). Potent and specific genetic interference by double-stranded RNA in *Caenorhabditis elegans*. Nature *391*, 806–811.

Francis, R., Barton, M.K., Kimble, J., and Schedl, T. (1995). *gld-1*, a tumor suppressor gene required for oocyte development in *Caenorhabditis elegans*. Genetics *139*, 579–606.

Gaulden, M.E., and Carlson, J.C. (1951). Cytological effects of colchicine on the grasshopper neuroblast *in vitro* with special reference to the origin of the spindle. Exp. Cell Res. *2*, 415–433.

Gönczy, P., Schnabel, H., Kaletta, T., Amores, A.D., Hyman, T., and Schnabel, R. (1999). Dissection of cell division processes in the one cell stage *Caenorhabditis elegans* embryo by mutational analysis. J. Cell Biol. *144*, 927–946.

Greenstein, D., Hird, S., Plasterk, R.H.A., Andachi, Y., Kohara, Y., Wang, B., Finney, M., and Ruvkun, G. (1994). Targeted mutations in the *Caenorhabditis elegans* POU homeo box gene *ceh-18* cause defects in oocyte cell cycle arrest, gonad migration, and epidermal differentiation. Genes Dev. *8*, 1935–1948.

Hall, D.H., Winfrey, V.P., Blaeuer, G., Hoffman, L.H., Furuta, T., Rose, K.L., Hobert, O., and Greenstein, D. (1999). Ultrastructural features of the adult hermaphrodite gonad of *Caenorhabditis elegans*: relations between the germ line and soma. Dev. Biol. *212*, 101–123.

Hardwick, K.G., Li, R., Mistrot, C., Chen, R.-H., Dann, P., Rudner, A., and Murray, A.W. (1999). Lesions in many different spindle components activate the spindle checkpoint in budding yeast *Saccharomyces cerevisiae*. Genetics *152*, 509–518.

Hodgkin, J. (1997). Genetics. In: *C. elegans* II, ed. D. Riddle, T. Blumenthal, B. Meyer, and J. Preiss, Cold Spring Harbor, NY: Cold Spring Harbor Laboratory, 881–1047.

Hoyt, M.A., Totis, L., and Roberts, B.T. (1991). *S. cerevisiae* genes required for cell cycle arrest in response to loss of microtubule function. Cell *66*, 507–517.

Hwang, L.H., Lau, L.F., Smith, D.L., Mistrot, C.A., Hardwick, K.G., Hwang, E.S., Amon, A., and Murray, A.W. (1998). Budding yeast Cdc20: a target of the spindle checkpoint. Science *279*, 1041–1044.

Isnenghi, E., Cassada, R., Smith, K., Denich, K., Radnia, K., and von Ehrenstein, G. (1983). Maternal effects and temperature-sensitive period of mutations affecting embryogenesis in *C. elegans*. Dev. Biol. *98*, 465–480.

Kilmartin, J.V., Wright, B., and Milstein, C. (1982). Rat monoclonal anti-tubulin antibodies derived by using a new non-secreting rat cell line. J. Cell Biol. *93*, 576–582.

Kim, S.H., Lin, D.P., Matsumoto, S., Kitazono, A., and Matsumoto, T. (1998). Fission yeast Slp1: an effector of the Mad2-dependent spindle checkpoint. Science *279*, 1045–1047.

Kitagawa, R., and Rose, A.M. (1999). Spindle assembly checkpoint components are essential in *Caenorhabditis elegans*. Nat. Cell Biol. *1*, 514–521.

Klein, F., Mahr, P., Galova, M., Cuonomo, S.B.C., Michaelis, C., Nairz, K., and Nasmyth, K. (1999). A central role for cohesins in sister chromatid cohesion, formation of axial elements, and recombination during yeast meiosis. Cell *98*, 91–103.

Kramer, J., French, R.P., Park, E., and Johnson, J.J. (1990). The *Caenorhabditis elegans rol-6* gene, which interacts with the *sqt-1* collagen gene to determine organismal morphology, encodes a collagen. Mol. Cell. Biol. *10*, 2081–2090.

Krause, M. (1995). Transcription and translation. In: Methods in Cell Biology, ed. H. Epstein and D. Shakes, San Diego, CA: Academic Press, 483–512.

Li, R., and Murray, A.W. (1991). Feedback control of mitosis in budding yeast. Cell *66*, 519–531.

Li, X., and Nicklas, R.B. (1995). Mitotic forces control a cell cycle checkpoint. Nature *373*, 630–632.

Mahadevan, L.C., Willis, A.C., and Barratt, M.J. (1991). Rapid histone H3 phosphorylation in response to growth factors, phorbol esters, okadaic acid, and protein synthesis inhibitors. Cell *65*, 775–783.

Matthews, L.R., Carter, P., Thierry-Mieg, D., and Kemphues, K. (1998). ZYG-9, a *Caenorhabditis elegans* protein required for microtubule organization and function, is a component of meiotic and mitotic spindle poles. J. Cell Biol. *141*, 1159–1168.

McCarter, J., Bartlett, B., Dang, T., and Schedl, T. (1997). Soma-germ cell interactions in *Caenorhabditis elegans*: multiple events in germline development require the somatic sheath and spermathecal lineages. Dev. Biol. *181*, 121–143.

McCarter, J., Bartlett, B., Dang, T., and Schedl, T. (1999). On the control of oocyte meiotic maturation and ovulation in *C. elegans*. Dev. Biol. *205*, 111–128.

Mello, C., and Fire, A. (1995). DNA transformation. In: Methods in Cell Biology, ed. H. Epstein and D. Shakes, San Diego, CA: Academic Press, 452–482.

Morgan, D.O. (1997). Cyclin-dependent kinases: engines, clocks, and microprocessors. Annu. Rev. Cell Dev. Biol. *13*, 261–291.

Nasmyth, K. (1999). Separating sister chromatids. Trends Biochem. Sci. *24*, 98–104.

Neer, E.J., Schmidt, C.J., Nambudripad, R., and Smith, T.F. (1994). The ancient regulatory-protein family of WD-repeat proteins. Nature *371*, 297–300.

Nonet, M.L., Staunton, J.E., Kilgard, M.P., Fergestad, T., Hartwieg, E., Horvitz, H.R., Jorgensen, E.M., and Meyer, B.J. (1997). *Caenorhabditis elegans rab-3* mutant synapses exhibit impaired function and are partially depleted of vesicles. J. Neurosci. *17*, 8061–8073.

O'Connell, K.F., Leys, C.M., and White, J.G. (1998). A genetic screen for temperature-sensitive cell-division mutants of *Caenorhabditis elegans*. Genetics *149*, 1303–1321.

Plasterk, R.H.A. (1995). Reverse genetics: from gene sequence to mutant worm. In: Methods in Cell Biology, ed. H. Epstein and D. Shakes, San Diego, CA: Academic Press, 59–80.

Rieder, C.L., Schultz, A., Cole, R., and Sluder, G. (1994). Anaphase onset in vertebrate somatic cells is controlled by a checkpoint that monitors sister kinetochore attachment to the spindle. J. Cell Biol. *127*, 1301–1310.

Rose, K.L., Winfrey, V.P., Hoffman, L.H., Hall, D.H., Furuta, T., and Greenstein, D. (1997). The POU gene *ceh-18* promotes gonadal sheath cell differentiation and function required for meiotic maturation and ovulation in *Caenorhabditis elegans*. Dev. Biol. *192*, 59–77.

Sadler, P.L., and Shakes, D.C. (2000). Anucleate *Caenorhabditis elegans* sperm can crawl, fertilize oocytes and direct anterior-posterior polarization of the 1-cell embryo. Development *127*, 355–366.

Sigrist, S., Jacobs, H., Stratmann, R., and Lehner, C.F. (1995). Exit from mitosis is regulated by *Drosophila fizzy* and the sequential destruction of cyclins A, B and B3. EMBO J. *14*, 4827–4838.

Sluder, G. (1979). Role of spindle microtubules in the control of cell cycle timing. J. Cell Biol. *80*, 674–691.

Sondek, J., Bohm, A., Lambright, D.G., Hamm, H.E., and Sigler, P.B. (1996). Crystal structure of a G-protein beta gamma dimer at 2.1A resolution. Nature *379*, 369–374.

Sternberg, P.W., and Horvitz, H.R. (1989). The combined action of two intercellular signaling pathways specifies three cell fates during vulval induction in *C. elegans*. Cell *58*, 679–693.

Strome, S. (1986). Immunofluorescence visualization of germ-line-specific cytoplasmic granules in embryos, larvae, and adults of *Caenorhabditis elegans*. J. Embryol. Exp. Morphol. *97*(suppl), 15–29.

Strome, S., and Wood, W.B. (1982). Immunofluorescence visualization of germ-line-specific cytoplasmic granules in embryos, larvae, and adults of *C. elegans*. Proc. Natl. Acad. Sci. USA *79*, 1558–1562.

Sulston, J.E., and Horvitz, H.R. (1977). Post-embryonic cell lineages of the nematode, *Caenorhabditis elegans*. Dev. Biol. *56*, 110–156.

Thompson, J.D., Higgins, D.G., and Gibson, T.J. (1994). CLUSTAL W: improving the sensitivity of progressive multiple sequence alignment through sequence weighting, position specific gap penalties and weight matrix choice. Nucleic Acids Res. *22*, 4673–4680.

Uhlmann, F., Lottspeich, F., and Nasmyth, K. (1999). Sister-chromatid separation at anaphase onset is promoted by cleavage of the cohesin subunit Scc1. Nature *400*, 37–42.

Wall, M.A., Coleman, D.E., Lee, E., Iniguez-Lluhi, J.A., Posner, B.A., Gilman, A.G., and Sprang, S.R. (1995). The structure of the G protein heterotrimer Gi alpha 1 beta 1 gamma 2. Cell *83*, 1047–1058.

Ward, S., and Carrel, J.S. (1979). Fertilization and sperm competition in the nematode *Caenorhabditis elegans*. Dev. Biol. *73*, 304–321.

Ward, S., Robertes, T.M., Strome, S., Pavalko, F.M., and Hogan, E. (1986). Monoclonal antibodies that recognize a polypeptide antigenic determinant shared by multiple *Caenorhabditis* sperm-specific proteins. J. Cell Biol. *102*, 1778–1786.

Williams, B.D. (1995). Genetic mapping with polymorphic sequence-tagged sites. In: Methods in Cell Biology, ed. H. Epstein and D. Shakes, San Diego, CA: Academic Press, 81–96.

Yamashita, Y.M., Nakaseko, Y., Kumada, K., Nakagawa, T., and Yanagida, M. (1999). Fission yeast APC/cyclosome subunits, Cut20/Apc4 and Cut23/Apc8, in regulating metaphase-anaphase progression and cellular stress responses. Genes Cells *4*, 445–463.

Yandell, M.D., Edgar, L.G., and Wood, W.B. (1994). Trimethylpsoralen induces small deletion mutations in *Caenorhabditis elegans*. Proc. Natl. Acad. Sci. USA *91*, 1381–1385.

Yen, T.J., Compton, D.A., Wise, D., Zinkowski, R.P., Brinkley, B.R., Earnshaw, W.C., and Cleveland, D.W. (1991). CenP-E, a novel human centromere-associated protein required for progression from metaphase to anaphase. EMBO J. *10*, 1245–1254.

Yu, H., Peters, J.-M., King, R.W., Page, A.M., Hieter, P., and Kirschner, M.W. (1998). Identification of a cullin homology region in a subunit of the anaphase-promoting complex. Science *279*, 1219–1222.

Zachariae, W., and Nasmyth, K. (1999). Whose end is destruction: cell division and the anaphase-promoting complex. Genes Dev. *13*, 2039–2058.

Zachariae, W., Shevchenko, A., Andrews, P.D., Ciosk, R., Galova, M., Stark, M.J.R., Mann, M., and Nasmyth, K. (1998). Mass spectrometric analysis of the anaphase-promoting complex from yeast: identification of a subunit related to cullins. Science *279*, 1216–1219.